Final Technical Report
Grant Award Number: G12AP20012

Project Title:
Imaging Shallow Crustal Structure in the Upper Mississippi Embayment using Local Earthquake Data

Principal Investigators:
Shu-Chioung C. Chiu (PI); scchiu@memphis.edu; (901) 678-4915
Charles A, Langston (Co-PI), clangstn@memphis.edu; (901) 678-4869
Jer-Ming Chiu (Co-PI); jerchiu@memphis.edu; (901) 678-4839
Mitch W ithers (Co-PI), mwithers@memphis.edu; (901) 678-4940
Center for Earthquake Research and Information
The University of Memphis
Memphis, TN 38152
FAX: (901) 678-4734

Award Term
January 1, 2012 – March 31, 2014

Submitted Date
June 29, 2014

Table of Contents

Abstract

In this research project, we utilize 1-D pseudo-imaging profiling technique to analyze reflected P- and S-wave and transmitted Sp waves shown on New Madrid micro-earthquake waveform data in an attempt to mapping common reflectors and determine velocity structure of deep unconsolidated sediments in the upper Mississippi embayment. This method capitalize on the facts that the sediments have very low velocity and relatively high Q so that first reverberations of P- and S- wave, transmissions Sp waves and high-frequency resonances can be observed and identified from displacement seismograms. Our hypothesis is that micro-earthquake waveform data can provide an accurate view of wave propagation mechanisms. Both earthquake waveforms and geotechnical data can be jointly modeled to produce a much more accurate sediments structure and to predict wave propagation effects. These studies result in average velocities in a range of 1.95 to 2.42 km/s for P wave and 0.60 to 0.73 km/s for S wave in the deep sediments beneath stations. Although velocities vary slightly under stations, P-PpPhp and S-SsShs times appear linearly proportional to corresponding sediment depths, which provides an average velocity of 2.0 km/s for P-wave and 0.7 km/s for S-wave in the first-order least-squares sense for the entire sediments in upper Mississippi Embayment. Results of this project have been organized into two papers. They are attached is this report. Paper #1 is entitled "Imaging Shallow Crustal Structure in Upper Mississippi Embayment Using Local Earthquake Waveform Data". Paper #2 is entitled "Transfer Function and its Implication at the CUSSO Borehole Array in Southwestern Kentucky by Using Micro-earthquake Waveform Data".

Introduction

The New Madrid Seismic Zone (NMSZ) is the most seismically active region in the United States east of the Rocky Mountains. More than 10,000 earthquakes were recorded instrumentally and archived in an earthquake catalog at Center for Earthquake Research and Information (CERI), University of Memphis since late 1974. Evidence of widely distributed liquefaction, recent paleoseismological studies, and repeatedly and relatively concentrated seismicity reveal that there are potential to have damaging earthquakes in the NMSZ. Site conditions of the sediments in the embayment are classified as D (Vs of 180 m/s to 360 m/s) or E (Vs < 180 m/s) in the National Earthquake Hazards Reduction Program (NEHRP FEMA-450-1/2003). The characteristics of the extremely low P- and S- wave velocities in its near-surface soft soils and the large impedance contrast between the unconsolidated sediments and the underlain Paleozoic bedrock constitute an environment that has a significant effect on earthquake ground motion by amplifying and prolonging the shaking duration during a large earthquake. For example, ground motions amplified by Ohio River deposits caused approximately $3 million in damage at Marysville, KY, from the magnitude 5.2 Sharpsburg, KY, earthquake in 1980. Recently, displacement seismograms recorded by sensors located on bedrocks and at the surface in the Central US Seismological Observatory (CUSSO) vertical array for a magnitude 4.7 Greenbrier, Arkansas earthquake and the magnitude 9.0 Japan earthquake showed that ground motions have been amplified and prolonged shaking duration. Waveforms become more complicate and contain higher frequencies at the surface recordings as waves traveling through unconsolidated sediments. Many cities in the central US, such as Memphis, Tennessee, St. Louis, Missouri, and Paducah, Kentucky, are built on top of soft soils and deep sediments along the Mississippi and Ohio Rivers. Recent studies suggest that geotechnical data such as Vertical Seismic Profiling (VSP), Seismic Cone Penetration Tests (SCPT) or a simple Vs30 model may not properly predict site responses nor yield wave propagation effects due to the velocity averaging used over complicated sediments structure. Our hypothesis is that both earthquake waveform and geotechnical data can be jointly modeled to produce a much more accurate model and to predict wave propagation effects. We apply 1-D pseudo-imaging profiling method to reflections and transmissions shown on local earthquake waveform data from existing facilities – Cooperative New Madrid Seismic Network (CNMSN) and CUSSO, as well as a temporary deployment data to examine site responses in the NMSZ and to solve velocity model for unconsolidated sediment structures directly inferring to seismic wave propagation effects.

Hypothesis

The hypothesis of this research is that micro-earthquake displacement waveform can provide an accurate view of wave propagation mechanism. A corollary of this hypothesis is that both earthquake waveforms and geotechnical data can be jointly modeled to produce a much more reliable model of earth structure and to predict the wave propagation effect.

Methodology - 1-D pseudo-imaging profiling

We apply 1-D pseudo-imaging technique to P- and S- reflections (PpPhp and SsShs) and Sp transmissions displayed on local earthquake displacement seismograms for computing NMO migrated seismic depth section to solve first-order velocity structure in the upper Mississippi embayment. Details of this method can be found in Chiu and Langston (2009); while we summarize here. Processes consist of (1) constructing an appropriate velocity model; (2) calculating Normal MoveOut (NMO) correction; (3) converting time series of reflection and transmission to a function of depth; and (4) identifying common reflectors, correlating to stratigraphic interfaces and interpreting. NMO correction is performed by (1) calculating two-way travel times for reflected P- and S- wave, and one-way differential travel times between P- and S- wave for transmitted Sp waves as a function of interface depth using actual ray parameter obtained from the earthquake source to station and earth model; (2) re-sampling travel times to an equal depth interval of 0.01 km; and (3) converting time series to a function of depth by applying NMO corrections. Thus, interpretation of 1-D seismic migrated depth section can be made in a similar way to the interpretation of the traditional seismic reflection profile.

Velocity Model in Mississippi Embayment

P-wave velocity, S-wave velocity and density are required parameters for computations in the 1-D pseudo-imaging method. However, deep acoustic well logs in this region are distributed sparsely; meanwhile, there are currently no extensive loggings for either bulk density or S-wave velocity; except, slowness measurements for S-wave were conducted in a deep borehole drilling at the CUSSO operated by University of Kentucky since 2008. As shown by logging data, P-wave velocity shows considerable heterogeneity with depth but attains an average of 1.8 - 2.0 km/s below water table (e.g., Liu *et. al.,* 1997; Chiu and Langston, 2009; Chiu *et. al.,* 2014a). The CUSSO well logging data show similar variability in Vp profile; though, borehole Vs profile from direct measurements appears about half slower down to ~ 0.3 km (Chiu *et. al.,* 2014a). In contrast to an average S-wave velocity of 0.6 – 0.7 km/s in the NMSZ, an average S-wave velocity of ~0.4 km/s is acquired from the CUSSO borehole logging data. This contradicts to 0.6 km/sec resolved from the waveforms observed at the surface and base of the CUSSO borehole array (Chiu *et. al.,* 2014a). In this manner, we are not certain about the credibility of drilling measurements for S-wave at CUSSO array. Perhaps, the most reliable and detailed data is the acoustic well log taken at Wilson 2-14 in February 2001, near Kaiser, Arkansas. Dorman and Smalley (1994) suggested an empirical approach to derive both parameters - S-wave velocity and bulk density - from acoustic slowness data in the well logs using a Nafe-Drake sediment model (Nafe and Drake, 1957). The exponent, n, relating shear-wave velocity to porosity, can be 5.6 for the embayment sediments in the NMSZ (Langston, 2003a).

Because the depth variation of physical properties of unconsolidated sediments is not dramatic in the region, we assume that the acoustic well log data of the Wilson 2-14 can be used and scaled to depth of sediments beneath each station; S-wave velocity is derived using an empirical approach. We also assume that the acoustic well log data of the Dow Chemical/Wilson #1 can represent Paleozoic rocks assuming Poisson's solid throughout the entire basin. An average Vp of 6.0 km/s and Vs of 3.5 km/s are found from well log data of Dow Chemical/Wilson #1. Accordingly, we construct a thin-layered earth model consisting of detailed acoustic variations in the Phanerozoic sediments down to depth of ~4 km. We refer it to the detailed velocity model in this research project. Nonetheless, the Wilson 2-14 well model might not be the best in representing structure beneath station; and/or laterally heterogeneous structure might exist in close distances. Paleozoic sedimentary rock may or may not be a Poisson's solid. Two velocity models are considered here. One is the detailed model. For the other model, P- and S-

wave velocity structures have been smoothed and simplified to facilitate the calculation of travel time curves and synthetic seismograms. High frequency scattering waves have been smoothed by using a causal Butterworth bandpass filter with corner frequencies of 0.5 and 5 Hz for P- and Sp-wave and 0.5 and 10 Hz for S-wave such that all waves exhibit similar frequency waveforms. We will allow small adjustments to Vp and Vs in the NMO migration process so that reflection and transmission effects can be attributed to common reflectors among P-, S-, and Sp-waves, from which a velocity model can be determined.

Waveform Data Selection

We search extensively the entire CERI earthquake catalog to select events having high signal–to-noise ratios so that seismic phases can be identified and their arrival time differences can be estimated. To avoid complication in the wave propagation effects, we also choose events close to the station to assure simple ray paths and simple wave shapes. P-S arrival time needs 3 s or more to resolve a reflector at 4 to 4.5 km. In the application of earthquake data, we need consider all aspects, e.g. magnitude, source-receiver offset, azimuthal variation, and hypocenter depth. Pre-stacking selected waveforms may be necessary.

Waveform Data Pre-processing

Data pre-processing involves (1) selecting microearthquake waveforms with clear P-, S- and Sp-phases; (2) correcting DC offset and trend, changing all times with respect to origin time; (3) removing instrument response; (4) integrating to displacement; (5) rotating along the great circle; (6) extracting P- and S-wave coda (include reflected waves and converted Sp waves).

Conclusions

Pre-stacking P- and S-wave coda including reflected waves (PpPhp and SshSs) and converted Sp-waves were used to perform a 1-D NMO migration in an attempt to mapping common reflectors associated with stratigraphic interfaces and to solve an average velocity model for unconsolidated sediments under selected stations in the upper Mississippi Embayment. This technique had been successfully applied to the CNMSN stations at PARM, Stahl Farm, Missouri and PENM, Penman Portageville, Missouri (Chiu and Langston, 2009), all other CNMSN broadband and a short-period stations (Chiu *et. al.*, 2012), the CUSSO borehole array data as well as a temporary station CUKY co-sited at the top of CUSSO in southwestern Kentucky (Chiu *et. al.*, 2014a). Despite polarity differences among P-, S-, and Sp-wave, this technique demonstrates that common reflectors in the deep sedimentary section can be simultaneously identified among three wave types. There were excellent correlations associated with the base of the upper Cretaceous/Holocene Mississippi Embayment Super group, the base of Knox group, possible low-velocity Elvins shale zone, high-velocity Bonneterre Formation Marker and probable crystalline basement at 4.0 - 4.5 km depth, which were also reported in previous reflection/refraction experiments in this region. In addition, it is interesting to notice that the high frequency Sp waves are converted at shallower depths and the base of unconsolidated sediments while relatively long-period Sp waves are converted at deeper interfaces. These observations imply that multiple Sp-wave conversions occur in the Mississippi Embayment, starting from the deeper interfaces.

These studies find average velocities of deep unconsolidated sediments in a range of 1.95 to 2.42 km/s for P-wave and in a range of 0.60 to 0.73 km/s for S-wave. Meanwhile, P-PpPhp (S-SsShs) time seems linearly proportional to the sediment thickness. It gives an average velocity of 2.0 km/s for P-wave (0.7 km/s for S-wave) in the first-order least-squares sense for deep unconsolidated sediments in upper Mississippi Embayment. These velocity models are useful to other seismological studies; such as near-surface soil structure modeling of high-frequency site responses displayed on local earthquake displacement seismograms.

Results of this project have been organized into two papers currently in review for publication at the Bulletin Seismological Society of America (2014). They are attached below.

Attachment 1. Imaging Shallow Crustal Structure in Upper Mississippi Embayment Using Local Earthquake Waveform Data, (2014), submitted to *Bull. Seism. Soc. Am.*, Chiu, S.C; C.A. Langston, J.M. Chiu, and M. Withers.

Attachment 2. Transfer Function and its Implications at the CUSSO Borehole Array in Southwestern Kentucky using Microearthquake Waveform Data, (2014), submitted to *Bull. Seism. Soc. Am.*, Chiu, S.C., J.M. Chiu, C.A. Langston, Z. Wang, and E. Woolery.

Acknowledgments

We would like to express our greatest gratitude to the anonymous reviewers for their detailed review, valuable comments and suggestions, which are incorporated in the manuscript. The Seismic Analysis Code (Goldstein et. al., 1996) and GMT (Wessel and Smith, 1998) are used for much of data processing, analyses, and preparing figures and are gratefully acknowledged. This research is supported by the U.S. Geological Survey, Department of Interior, under NEHRP grant award numbers G09AP00096 and G12AP20012 (University of Memphis) and G09AP000126 (University of Kentucky) and the Center for Earthquake Research and Information, University of Memphis. The views and conclusions contained in this document are those of the authors and should not be interpreted as necessarily representing the official policies, either expressed or implied, of the U.S. government.

Attachment 1

Imaging Shallow Crustal Structure in Upper Mississippi Embayment Using Local Earthquake Waveform Data

by

Shu-Chioung Chi Chiu, Charles A. Langston, Jer-Ming Chiu, and Mitch Withers
Center for Earthquake and Research and Information
The University of Memphis, Memphis, TN 38152

Abstract

We utilize the characteristic features of primary P- and S-wave coda, their reflections, and transmitted Sp waveforms converted at the base of unconsolidated sediments from local microearthquake data and perform pre-stacking 1-D NMO migration in an attempt to image common reflectors and to resolve velocity structure for unconsolidated sediments in the upper Mississippi Embayment. The observed travel times of the reflected P- and S-wave as well as converted Sp waves provide important constraints on identifying reflectors and determining velocity model in the deep sediment column. We analyze and model local earthquake waveform data collected by the existing Cooperative New Madrid Seismic Network (CNMSN) for all broadband and a short-period stations, data from a deep vertical seismic array, Central US Seismological Observatory (CUSSO) operated by he University of Kentucky (UKY), and data from selected temporary broadband stations within embayment. Despite polarity differences among P-, S-, and Sp-waves this technique demonstrates that common reflectors in the deep sedimentary section can be simultaneously mapped using these three wave types. These reflectors have excellent correlations with the base of the upper Cretaceous/Holocene Mississippi Embayment Super Group, the base of Knox Group, possible a localized low-velocity Elvins shale zone, high-velocity Bonneterre Formation Marker, and a probable crystalline basement at 4.0 - 4.5 km depth, which were also reported previously from the reflection/refraction experiments conducted by Hamilton and Zoback (1982) and Mooney *et al.,* (1983). These studies conclude that average velocities in a range from 1.95 to 2.42 km/s for P-wave and 0.60 to 0.73 km/s for S-wave can represent the velocity structure of deep sediments in the New Madrid Seismic Zone (NMSZ). Although velocities slightly vary beneath stations, P-PpPhp and S-SsShs differential times appear linearly proportional to sediment thicknesses. It gives an average 1-layer sediment structure of Vp 2.0 km/s and Vs 0.7 km/s at the first-order least-squares approximation for the upper Mississippi Embayment. This study indicates that S-P arrival time difference must be ~3 s or longer to resolve reflector at about 4 km.

The method used in this study will enable us to empirically examine site amplification of low-strain seismic waves independent of geotechnical field methods. The use of high-frequency (0.2-20 Hz) earthquake body waveforms can yield structure models that can be employed to estimate site specific amplification for future large ground motions due to strong earthquakes in the upper Mississippi Embayment. Velocity models can be implemented in high frequency simulations to characterize seismic wave propagation and attenuation in the region.

Introduction

The NMSZ is the most seismically active region in the United States east of the Rocky Mountains (Johnston and Schweig, 1996). More than 10,000 earthquakes have been recorded instrumentally and archived at the Center for Earthquake Research and Information (CERI) since late 1974 (Figure 1). The Mississippi Embayment overlies the entire NMSZ and is filled with up to 1 km of upper Cretaceous-to-

recent sediments at the latitude of Memphis, Tennessee (~35°N) (Stearn, 1957). Geological evidences suggest a recurrence interval of approximate 500 years for large magnitude earthquakes in the region (Kelson *et al.,* 1996; Turttle and Schweig, 1999; Turttle *et. al.,* 2000). Evidences of widely distributed liquefaction (Nuttli, 1973; Johnston and Schweig, 1996; Tuttle *et. al*., 2000), recent Paleoseismology studies (Tuttle and Schweig 1999), and repeated and relatively concentrated seismicity have heightened the potential of damaging earthquakes in the NMSZ. Categorized by averaging shear wave velocity in the uppermost 30 m of loose soils, i.e. Vs30, site conditions of the embayment (Street, *et. al*, 2002; Williams, *et. al*., 2003) are classified as either D (Vs of 180 m/s to 360 m/s) or E (Vs < 180 m/s) (FEMA-450-1, 2003) in the National Earthquake Hazards Reduction Program (NEHRP). The characteristics of large impedance contrast between the unconsolidated sediments and the underlying Paleozoic bedrock, and the extremely low shear wave velocity in the near-surface soils constitute an environment that has a significant effect on earthquake ground motions by amplifying and prolonging shaking duration during a major earthquake (Jemberie and Langston, 2005; Langston *et. al.,* 2005).

It is evident that the seismic response of thick sediments in the upper Mississippi Embayment should be a primary target concerning earthquake hazard assessment in the central USA. For example, ground motions amplified by loose Ohio River deposits have caused approximate $3 million of damages at Marysville, KY, from the magnitude 5.2 Sharpsburg, KY, earthquake in 1980. Recent displacement seismograms recorded by sensors located on bedrocks and at the surface in the CUSSO borehole array from the February 28, 2011, magnitude 4.7 Greenbrier, Arkansas earthquake and the March 11, 2011, magnitude 9.0 Japan earthquake showed that ground motions were amplified and shaking duration was prolonged. Waveforms became more complicate and contained higher frequencies shown on the surface recordings due to reflected and transmitted waves generated in the complex structure of the unconsolidated sediments as waves propagation from bedrocks to the surface (Mclntyre *et. al.*, 2011). Recent study reveals that the near-surface amplification may reach to as large as twelve times due to the existence of extremely low-velocity soft soils (Chiu *et. al.*, 2014). Many communities in the central US, such as Memphis, Tennessee, St. Louis, Missouri, and Paducah, Kentucky, are built on top of soft soils along the Mississippi and Ohio Rivers. Observations from other parts of the world have also shown the influence of shallow soil structure to the characteristics of ground motions induced by great earthquakes, e.g. the 1988 Armenia, 1989 Loma Prieta, 1994 Northridge, 1995, Mexico, 1999 Chi-Chi, Taiwan, and 2001 Gujurat, India. These examples highlight the urgent need of understanding the site response of unconsolidated sediments and soft soils in the NMSZ and, consequently, the potential impact on earthquake damage and casualty.

Although acoustic well log data provide direct measurements of physical properties for sediments of the Mississippi Embayment, structures shallower than 80 m are usually not logged because of the well casing needed to stabilize wet soils in the embayment environment. The seismic reflection/refraction technique averages travel times over 10's to 100's meters. The results from geotechnical field experiment such as the Vertical Seismic Profiling (VSP) show that Vs profiles have little variations while Vp increases rapidly to the water table at ~10 m depth and attains an average of 1.8 to 2.0 km/s below the water table (Liu *et. al.,* 1997). Nevertheless, well log data may miss a major impedance interface(s) because of averaging incorporated in logging sampling. In other words, the velocities of the deep unconsolidated sediments and shallow soft soils are often uncertain even though velocities are essential to earthquake hazards assessment and the enhancement of seismic regulations for critical facilities, new buildings and structures.

Previous studies related to the upper Mississippi Embayment

Extremely low shear wave velocities are observed in near-surface soils (Romero and Rix, 2000; Schneider *et. al.*, 2001; Rix *et. al.*, 2002; Langston, 2003a & 2003b; Street *et. al.*, 2004; Ge, 2005; Lin, 2008a&b; Chiu and Langston, 2011). Controlled source surveys have been conducted in the Mississippi Embayment, including small- and large- scale reflection/refraction experiments, e.g. Hamilton and Zoback, 1982; Mooney *et. al.*, 1983; Nelson and Zhang, 1991; Catchings, 1999; Street *et. al.*, 2002; Langston *et. al.*, 2005. Geotechnical experiments such as Vertical Seismic Profiling (VSP) (Liu *et. al.*,

1997) and seismic cone penetration tests (SCPT) (Schneider *et. al.*, 2001) have been carried out in this area. Acoustic well logs have been studied by a number of investigators to place constraints on the location of the base of unconsolidated sediments (e.g., Van Arsdale and Tenbrink, 2000) and to infer average velocity model for earthquake location and tomography (e.g., Gao, 1999; Vlahovic *et. al.,* 2000) in this region.

A large-scale reflection/refraction survey conducted by Mooney *et al.*, (1983) in upper Mississippi Embayment showed Vp 1.8 km/s and Vs 0.6 km/s for unconsolidated sediments. 1-D P- and S-wave determinations using PANDA data collected in the central NMSZ area during 1988-1991 also showed a Vp of 1.8 km/s and Vs of 0.65 km/s (Chiu *et. al.*, 1992). Dorman and Smalley (1994) studied the dispersion of low-frequency surface waves to determine a homogeneous 1-layer sediment structure and suggested that embayment sediments could be explained as Nafe-Drake type marine sediments. Bodin *et al.* (2001) investigated deep sediment resonances across the eastern embayment near Memphis and found an empirical relationship between velocity and thickness of the sediments. Langston (2003) applied a waveform modeling method to determine horizontally layered substructures beneath five short-period stations (HAWT, CWPT, and MLNT in Tennessee, MCAM in Missouri, and NNAR in Arkansas) and a broadband station (PEBM in Missouri). An array study using microseismic noise to determine the wave field composition found that the amplitude of the H/V peak did not give an accurate estimate of shear wave amplification since it depended on the slowness of incident waves (Langston *et. al*., 2009). The H/V peak near 4 s (0.25 Hz) period was composed of relatively high phase velocity Rayleigh and Love waves that were converted to near-vertically propagating shear waves in the thick unconsolidated sediments. We developed and performed 1-D NMO migration on reflections and transmissions shown on local earthquake body wave seismograms and resolved a first-order estimate of Vp 2.0 km/s and Vs 0.65 km/s for sediments structure in Stahl Farm and Penman Portageville, southeastern Missouri (Chiu and Langston, 2009). Later, we reaffirmed the 1-D imaging profiling technique by applying to earthquake waveform data recorded by stations - HICK near CUSSO and CUKY co-sited at CUSSO, and resolving Vp 2.0 km/s and Vs 0.6 km/s in southwestern Kentucky (Chiu *et. al.*, 2014). This result agreed with the waveforms observed at the surface and base of unconsolidated sediments in the CUSSO borehole array. Constrained by the differential travel times of reflected and transmitted waves, imaging profiles captured the prominent reflectors correlating well with the Cretaceous/Paleozoic boundary, the Bonneterre Formation Marker and the top of the Pre-Cambrian among P-, S- and Sp-waves (Chiu and Langston, 2009; Chiu *et. al.,* 2014). In addition, shallower reflectors at depths of 10, 30, 70, 120, 185, 265, 310, and 500 m could be seen on P- and SH–wave imaging profiles (Chiu *et. al.*, 2014), which were also reported in the seismic reflection/refraction experiment near CUSSO by UoM/UKY. In this report, we examine reflections and transmissions seismic waves shown on local earthquake seismograms and implement normal moveout (NMO) migration to identify common reflectors and determine velocity models of deep sediments in the upper Mississippi Embayment.

Hypothesis

The hypothesis of this research is that microearthquake displacement waveform can provide an accurate view of wave propagation mechanism. A corollary of this hypothesis is that both earthquake waveforms and geotechnical data can be jointly modeled to produce a much more reliable model of earth structure and to predict the wave propagation effect.

Methodology – 1-D pseudo-imaging profiling

This method capitalizes on the facts that the unconsolidated sediments have very low velocities and a relatively high Q so that the first reverberations of P and S (PpPhp and SsShs) waves can be observed and identified from the displacement seismograms. Observed first reflections of P- and S-wave and transmission Sp waves will place strong constraints on the identification of common reflectors and determination of velocity structure. Detailed discussions of this method can be found in Chiu and Langston (2009) and are summarized here. Basically, four steps are involved. They are (1) constructing an appropriate velocity model; (2) calculating two-way travel times and one-way travel time differences

between P- and S-wave using average interval velocities with appropriate ray parameters and earth model for P- and S-wave coda and Sp-wave; (3) applying a "Stretching" operator to convert time series to depth profile; and (4) identifying reflectors, correlating with stratigraphic interfaces, and interpreting. The NMO migration is performed as follows: (1) one-way differential travel times for transmitted Sp-wave, and two-way travel times for reflected P- and S-waves are calculated using actual ray parameter and a given earth model; (2) travel times are re-sampled to an equal depth interval of 0.01 km; and (3) time series of reflections and transmissions are converted to a function of depth by applying NMO correction. Pre-stacking of selected waveforms may be necessary.

Velocity Model in the Mississippi Embayment

P-wave velocity, S-wave velocity and density are the required parameters for computations in the 1-D pseudo-imaging profiling. However, deep acoustic well logs in this region are distributed sparsely; meanwhile, there are no extensive loggings in this region for either bulk density or S-wave velocity. In 2008, the UKY group conducted direct measurements of S-wave slowness at CUSSO. Vertical Seismic Profiles (VSP) in the embayment reveal that P-wave velocities show considerable heterogeneity with depth but attain an average of 1.8 - 2.0 km/s below water table while S-wave velocities have little variations (Liu et. al., 1997; Chiu et. al., 2014). The CUSSO well logging data shows similar variability in Vp; though, borehole Vs profile from direct measurements is about half slower down to the depth ~ 0.3 km (Chiu *et. al.,* 2014). In contrast to an average S-wave velocity of 0.6 – 0.7 km/s in the NMSZ, an average S-wave velocity of ~0.4 km/s is acquired from the CUSSO logging data. This contradicts to 0.6 km/s obtained by the differential travel times shown on seismograms at the surface and the base of the CUSSO array (Chiu *et. al.,* 2014). In this manner, the credibility of drilling measurements for S-wave velocities at CUSSO will need further investigation.

Perhaps, the most reliable and detailed data is the acoustic well log data taken at the Wilson 2-14 in February 2001, near Kaiser, Arkansas. Dorman and Smalley (1994) suggested an empirical approach to derive both parameters, S-wave velocity and bulk density, from acoustic slowness data in the well logs using a Nafe-Drake marine sediment model (Nafe and Drake, 1957). The exponent, n, relating shear-wave velocity to porosity, can be 5.6 for the embayment sediments in the NMSZ (Langston, 2003a). Because the depth variation of physical properties in unconsolidated sediments is not dramatic in the region, we assume that the acoustic well log data of the Wilson 2-14 can be used and scaled to the depth pertaining to sediments beneath each station; S-wave velocity is derived using an empirical approach. We also assume that the acoustic well log data of the Dow Chemical/Wilson #1 can represent Paleozoic rocks assuming Poisson's solid throughout the entire basin. An average Vp 6.0 km/s and Vs 3.5 km/s are found from the Dow Chemical/Wilson #1 well log data. Accordingly, we construct a thin-layered earth model consisting of detailed acoustic variations in the Phanerozoic sediments down to depth of ~4 km. We refer it as the detailed velocity model in this research project. Nonetheless, the Wilson 2-14 well model might not be the best in representing structure beneath station; and/or laterally heterogeneous structure might exist in close distances. Paleozoic sedimentary rocks may or may not be Poisson's solid. Two velocity models are considered here. One is the detailed model. For other model, P- and S-wave velocity structures are smoothed and simplified to facilitate the calculation of travel time curves and synthetic seismograms. High frequency scattering effects are smoothed by using a causal Butterworth bandpass filter with corner frequencies of 0.5 and 5 Hz for P- and Sp-wave, and 0.5 and 10 Hz for S-wave such that all waves exhibit similar frequency waveforms. We will allow small perturbations on Vp and Vs in the NMO migration process so that reflection and transmission effects can be attributed to common reflectors among P-, S-, and Sp-wave, from which a velocity model will be determined.

Seismic Data Selection and Data Processing

In the application of earthquake data, all aspects including source-receiver offset, azimuthal variation, hypocenter depth, and a velocity model have to be considered in order to estimate the NMO corrections for reflections and transmissions. Then, seismic depth section can be interpreted similar to that used in the traditional reflection seismology. Earthquakes must be large enough to generate sufficient

excitation of P- and S-wave reverberations with high signal–to-noise ratio beneath the station, so that direct and reverberating phases can be identified and their differential travel times can be estimated. Seismic waveforms from local microearthquakes may be complicated due to velocity heterogeneity in the embayment. Stacking of the waveform data is an effective approach to enhance signals and suppress scattered waves and noises. We search events close to the selected station to ensure simple wave propagation paths and simple wave shapes. However, the receiver should also be located at adequate distance to allow full separation of P reflections from converted Sp arrival that took place at the base of the unconsolidated Cretaceous sediments and deeper interfaces. Based on the CERI standard velocity model (Chiu *et. al.*, 1992), the basement reflection arrives at ~1.62 s after the primary P arrival on the vertical-component seismogram and at ~3.28 s after the primary S arrival on the transverse-component seismogram. Sp conversions on the vertical-component precede direct S by ~0.84 s. Thus, event S-P times must be ≥3 s to resolve reflectors at about 4 km depth.

The Seismic Analysis Code (SAC2000) (Goldstein and Minner, 1996) is used to correct for DC-offset, trend, instrument response and subsequent waveform analysis. Corrected velocity waveforms are integrated once to obtain ground displacements. A zero-phase trapezoidal band pass filter is applied with frequency limits of 0.01, 0.1, 40, and 50 Hz. Two horizontal components are then rotated along the great circle to radial and transverse orientations to facilitate the separation of P and SV motions from SH motions. We select a time window from displacement seismograms to extract P-, S-wave coda, and Sp-waves from vertical- and transverse-component with zero-time reference at the peak of the first pulse and polarity corrected such that their first-motion is downward to enable the reflected and transmitted phases in up-motion similar to the traditional reflection seismology. Time shift is determined by applying cross-correlation between waveforms. Finally, all waves are corrected with respect to the zero-time reference before they are stacked to implement the NMO correction.

Seismic Imaging Case Study

In an earlier study, we developed, tested and applied this technique to model the velocity structure of sediments beneath stations PARM and PENM in southeastern Missouri (Chiu and Langston, 2009). Then, we verified this technique by focusing on local earthquake data recorded by a temporary broadband station, CUKY, co-sited at the top of the deep borehole CUSSO array and a near-by station HICK. 1-D pseudo-imaging profiling was applied to perform NMO migration on displacement waveforms recorded at both stations. The results revealed that a horizontal layer of Vp 2.0 km/s and Vs 0.6 km/s could represent velocity structure of the deep unconsolidated sediments in southwestern Kentucky. This result reaffirmed that the suggested velocity model could explain the observations for P- and S-wave acquired at the surface and base of the CUSSO array (Chiu *et. al.,* 2014). Now, we extend our study to analyze and model waveform data collected by all CNMSN broadband stations including GLAT, GNAR, HALT, LNXT, LPAR, PEBM, and one short-period station MORT to explore velocity structure of sediments in upper Mississippi Embayment. Locations of stations and earthquake source parameters used in the study are listed in Tables1 and 2, and also shown in Figure 1. Results from this study are summarized in Table 3 and are described below.

GNAR

Because the depth variation of physical properties (e.g. density and porosity) of unconsolidated sediment is not dramatic in the region, we assume that the acoustic well log data of the Wilson 2-14 can be used and scaled to depth of sediments beneath the station, and the acoustic well log data of the Dow Chemical/Wilson #1 can represent Paleozoic and older structure throughout the entire basin. In such manner, P-wave velocity model for unconsolidated sediments is constructed by using acoustic well log data of the Wilson 2-14 with 100 layers of 7.62 m layer thickness, pertaining to the unconsolidated sediment depth beneath GNAR at Gosnell, Arkansas (Figure 1). We average P-wave slowness within each layer interval to produce equivalent layer slowness. S-wave velocity and bulk density are derived from acoustic slowness data by an empirical approach using a Nafe-Drake marine sediment model, with a constant relating shear-wave velocity to porosity being 5.6 for the embayment sediments in the NMSZ

(Langston, 2003a). P-wave velocity beneath the Cretaceous sediments is derived from the acoustic well log data of the Dow Chemical/Wilson #1 with 118 layers of 30.48 m layer thickness. Again, we average the P-wave slowness in each layer interval to produce equivalent layer slowness to preserve vertical travel time. S-wave velocity is computed by assuming a Poisson solid ($\sigma = 0.25$). Thus, a velocity model for the crust of ~4 km depth is constructed. We will refer such constructed velocity model as the detailed velocity model hereafter.

In the practice of reflection seismology, reflected phases are corrected for time corresponding to the vertical incidence from source to receiver. In the application of earthquake data, we need to consider all aspects of source-receiver offset, azimuthal variation, hypocenter depth, and a velocity model to estimate the magnitude of NMO corrections for reflections and transmissions. In our earlier study, we found that vertical incidence two-way travel time calculation is a good approximation to the actual travel time for travel path within unconsolidated sediments. However, travel time curves for deeper reflectors deviate more from the reference curve at zero offset as offset increases (Chiu & Langston, 2009). To minimize the effects of laterally heterogeneous velocity structure on the seismic wave shapes, we select events within a radius from 8 km to 14 km around GNAR with clear P, S, and Sp arrivals to ensure a better NMO corrections for reflections and transmissions. Selected events are listed in Table 2.

Pre-processed waveform data for radial-, transverse- and vertical- component (RTZ) are shown in Figure 2a. High frequency scattering effects are smoothed using a causal Butterworth bandpass filter with corner frequencies of 0.5 and 5 Hz for P- and Sp-wave and 0.5 and 10 Hz for S-wave such that all waves exhibit similar frequency waveforms. We select time windows for P-wave (back to Sp) from Z-component and S-wave from T-component including their reflected waves. Zero-time is chosen at the peak of each phase. Sp-waveform is time-reversed with the peak of the direct SV-phase arrival being the zero-time from Z-component. We extract P- and S- wave coda including the reflected and transmitted waves, and time-reversed Sp wave (Figure 2b). Nonetheless, structural model from the Wilson 2-14 well log might not be the best in representing structure beneath GNAR. Paleozoic sedimentary rocks may or may not be Poisson's solid. Two-way travel times for P- and S-wave coda and one-way differential travel times for Sp waves are computed by assuming a one-layer velocity model with a constant velocity of Vp 2.0 km/s and Vs 0.65 km/s for unconsolidated sediments of 762 m thickness overlain a half-space with a constant high-velocity of Vp 6.0 km/s and Vs 3.5 km/s for the Paleozoic sedimentary materials. P- and S-wave coda with respect to two-way travel times and Sp-wave with respect to one-way differential travel times are plotted in Figure 2c. Now, we re-sample time series into an equal depth interval of 0.01 km and convert time series into a function of depth to implement NMO migration for P-, S- and Sp-waves (Figure 2d). First motions for all phases are corrected to downward motions. Our hypothesis is that stacking waveforms can enhance energy of the reflected or transmitted waves generated from a common reflector and reduce the scattering due to structural heterogeneity. Image profiling is achieved by plotting pre-stacking NMO migration P- and S-wave coda and Sp-wave repeatedly (Figure 2e).

Constrained by the observed $t_{P\text{-}PpPhp,}$ $t_{S\text{-}SsShs\ and}$ $t_{S\text{-}Sp}$, a strong reflector emerges at the base of unconsolidated sediments associated with the Mississippi Embayment Super Group at depth 762 m among three wave types. Since P-S arrival time difference is shorter than 3 s, there is insufficient length of P-wave coda to resolve the structure in the Paleozoic sedimentary rocks. Nevertheless, the apparent reflectors in S imaging profile seem to correlate well with the low-velocity Elvins shale layer and the high-velocity Bonneterre Formation Marker in the deeper Paleozoic structure that were also reported by Hamilton and Zoback (1982). Common reflectors are indicated by tick marks. Depth scales are the same among four panels in Figure 2e. It is noticed that the Sp image profiling is spatially stretched due to the nature of the NMO migration. The converted Sp-wave from high-velocity deeper structure may have large incidence angles while P- and S- reflections inside low-velocity sediments travel in near vertical ray paths.

GLAT

GLAT is close to the dense seismicity in the NMSZ, in western Tennessee. Detailed P wave velocity model for unconsolidated sediments is constructed by using the acoustic well log data from

Wilson 2-14 and scaled to sediment depth with 79 layers of 10 m layer thickness, pertaining to the unconsolidated sediment depth of 790 m beneath GLAT (Figure 1). Detailed velocity model consists of P- and S-wave velocity profiles for unconsolidated sediments and velocity model for Paleozoic rocks obtained in a similar manner as described earlier. Selected events are selected and listed in Table 2 to ensure relatively simple wave propagation paths and simple wave shapes. Pre-processed and filtered three-component displacements are shown in Figure 3a. We extract P- and S-wave coda including reflected waves, and time-reversed Sp wave. Peaks of individual phase are chosen as the zero reference time to correct polarity of first motions to downward before stacking. Figure 3b shows imaging profiles made of pre-stacking NMO migration waveforms assuming a constant velocity of Vp 2.0 km/s and Vs 0.7 km/s for unconsolidated sediments of 790 m thickness overlying a half space of Vp 6.0 km/s and Vs 3.5 km/s for Paleozoic sedimentary rocks (the same format as Figure 2e). As constrained by the observed $t_{P-PpPhp}$, $t_{S-SsShs}$ and t_{S-Sp}, this technique demonstrates that consistent reflectors in the deep sedimentary section can be imaged commonly among three wave types. Strong reflectors are associated to the stratigraphic interfaces of Mississippi Super Group, low-velocity zone of Elvins shale and high-velocity Bonneterre Formation Marker in the deeper Paleozoic structure, which were reported earlier by Hamilton and Zoback (1982). So, an average Vp 2.0 km/s and Vs 0.7 km/s for unconsolidated sediments of thickness 790 m overlying a half-space with Vp 6.0 km/s and Vs 3.5 km/s for Paleozoic rocks are determined for the structure beneath GLAT.

HALT

HALT is a CNMSN broadband station at Halls, Tennessee. Detailed P wave velocity model for unconsolidated sediments is constructed by scaling the acoustic well log data of Wilson 2-14 to a depth 770 m with 77 layers of 10 m layer thickness, pertaining to the unconsolidated sediment depth beneath HALT (Figure 1). S-wave velocity profile for sediments and velocity model for Paleozoic sedimentary rocks are derived in the similar ways described earlier. Five close-by events are chosen and listed in Table 2. Pre-processed and filtered displacement waveforms are shown in Figure 4a. Figure 4b shows the seismic imaging profiling (the same format as Figure 2e) made of pre-stacking NMO migration waves assuming a one-layer constant velocity model of Vp 2.0 km/s and Vs 0.70 km/s in the unconsolidated sediments of 770 m depth overlying a half-space of Paleozoic sedimentary rocks with Vp 6.0 km/s and Vs 3.6 km/s. A clear reflector is located between Cretaceous sediments and Paleozoic rocks at depth of 770 m associated to the Mississippi Super Group. However, there are no clear reflectors associated to the Elvins shale and Bonneterre Formation Marker.

HENM

HENM is a broadband station, located at Henderson Mound, Missouri. Detailed P-wave velocity model for the unconsolidated sediments is constructed by scaling acoustic well log data of Wilson 2-14 to a depth 476 m with 100 layers of 4.76 m layer thickness. We process two waveforms for events listed in Table 2. Displacement waveforms are shown in Figure 5a. The seismic imaging depth section is generated by using a one-layer constant velocity model of Vp 2.1 km/s and Vs 0.65 km/s for the unconsolidated sediments of 476 m depth overlying a half-space of Vp 6.0 km/s and Vs 3.5 km/s for Paleozoic rocks shown in Figure 5b (the same format as Figure 2e). A clear reflector at depth 476 m can be associated with the interface between Cretaceous sediments and Paleozoic sedimentary rocks. Again, there are no clear reflectors associated with low-velocity Elvins shale and high-velocity Bonnetrree Formation Marker.

LNXT

LNXT is a CNMSN broadband station, located at Lenox, Tennessee where sediments thickness is 816 m (Figure 1). P-wave velocity profile is constructed by scaling well log data of Wilson's 2-14 to 100 layers with 8.16 m layer thickness. Five events are chosen (Table 2) and their waveforms are shown in Figure 6a. A seismic imaging depth section is generated assuming a one-layer constant velocity model with Vp 2.0 km/s, Vs 0.7 km/s for unconsolidated sediments of 816 m thickness overlying a half-space of

Paleozoic rocks with Vp 6.0 km/s and Vs 3.4 km/s (Figure 6b, the same format as in Figure 2e). A strong reflector is located between Cretaceous sediments and Paleozoic rocks at depth of 816 m that can be correlated to the Mississippi Super Group interface. There are also two reflectors that can be associated with the low-velocity Elvins shale zone and the high-velocity Bonneterre Formation Marker.

LPAR

LPAR is a CNMSN broadband station, located at Lepanto, Arkansas. The sediment depth beneath LPAR is 855m (Figure 1). P-wave velocity profile is constructed by scaling well log data from Wilson 2-14 to 100 layers with 8.55 m layer thickness. Four events are selected and listed in Table 2. Their pre-processed displacement seismograms are shown in Figure (7a). The NMO migration seismic section is constructed by using a one-layer constant velocity model with Vp 2.07 km/s and Vs 0.73 km/s for unconsolidated sediments of 855 m thickness overlying a half-space Paleozoic rocks with Vp 6.1 km/s and Vs 3.5 km/s as shown in Figure 7b (the same format as in Figure 2e). The imaging profiling shows strong reflectors that can be correlated to stratigraphic interfaces corresponding to the Mississippi Super Group (S) at depth 855m, dolomite layer at depth 1 km, and low-velocity Evins shale zone (E) on the top of the high-velocity Bonneterre Formation Marker (B) at 2.8 - 3.2 km.

PEBM

PEBM is a CNMSN broadband station, located at Pemiscot Bayou, Missouri. The sediment thickness is 749 m beneath the station. P-wave velocity profile is constructed by scaling the well log data of Wilson 2-14 to 100 layers with 7.49 m layer thickness. Displacement seismograms of five earthquakes (Table 2) are pre-processed and shown in Figure 8a. A migrated seismic imaging section is generated assuming a one-layer constant velocity model with Vp 1.95 km/s and Vs 0.70 km/s for unconsolidated sediments of 749 m thickness overlying a half-space of Paleozoic rocks of Vp 6.2 km/s and Vs 3.3 km/s (Figure 8b; the same format as in Figure 2e). Imaging profiles display strong reflectors that can be correlated to the Mississippi Super Group at depth of 749 m, high-velocity Bonneterre Formation Marker at ~3.2 km, and possible low-velocity Elvins shale layer. Imaging profiles for both P- and S-waves also show a basement at ~4 km.

MORT

Mort is one of the short-period stations in the CNMSN, located at Mooring, Tennessee. The sediment depth is 750 m (Figure 1). P-wave velocity profile is constructed by scaling the well log data of Wilson 2-14 to 75 layers with 10 m layer thickness. Displacement waveforms from two selected local earthquakes (Table 2) are shown in Figure 9a. Imaging profiling is constructed by using a one-layer constant velocity model with Vp 2.42 km/s and Vs 0.62 km/s for unconsolidated sediments of 750 m thickness overlying a half space of Paleozoic rocks with Vp 6.0 km/s and Vs 3.5 km/s. Imaging profiles (Figure 9b) display strong reflectors at depth 750 m associated to the stratigraphic Mississippi Super Group (S) among P-, S- and Sp- wave and at depth 1 km correlated to the dolomite layer between P- and S-wave. However, there is not sufficient length of P-wave coda to imaging reflectors deeper than 2 km. Again, it needs S-P arrival time about or greater than 3 s in order to resolve reflectors to a depth of 4 km. Low-frequency Sp waves do not appear as significant as shown on broadband seismograms due to the narrow bandwidth in instrument response. It seems that there are insufficient low-frequency information on short-period seismograms to image deeper structure in the Paleozoic rocks.

Results

All shallow crustal structural models described above are summarized in Table 3. The deep unconsolidated sediments can be represented by a one-layer constant velocity model with Vp in the range from 1.95 to 2.42 km/s and Vs from 0.60 to 0.73 km/s. Although they vary slightly, a first-order velocity model for deep unconsolidated sediments can be expressed in a least-squares determination of the curve that best describes the relationship between the expected and observed data by minimizing the sums of the squares of deviation between the observed and expected values. Taking advantage of the observed P- and

S-reflected waves and their travel time moveouts (P-to-PpPhp for P-wave and S-to-SsShs for S-wave) with respect to corresponding sediment thicknesses among stations, it provides an estimate of average velocity Vp 2.084 km/s (Figure 10a) and Vs 0.708 km/s (Figuer 10b) for a first-order one-layer velocity model of unconsolidated sediments in the upper Mississippi Embayment (Figure 10). This result agrees with the findings from seismic-reflection profiles (Hamiltom and Zoback, 1982) and the COCORP (Consortium for Continental Reflection Profiling) deep reflection survey (Nelson and Zhang, 1991) in the embayment. This may be one of the most unbiased estimators predicted by wave propagation effects. This study demonstrates that NMO migration P-, S-, and Sp-wave imaging profiles calculated from displacement seismograms including their reflections and transmissions may also be used to determine velocity model. These profiles show consistently common reflectors: The prominent reflector associated with the base of the embayment Super Group results from a large impedance contrast produced by low velocity, poorly consolidated upper Cretaceous classic sediments of the embayment Super Group lying above high–velocity lower Ordovician dolomites of the Knox Group; The reflector associated with the base of the Knox Group is excited by the transmission of seismic waves from the lower-velocity shale of the upper Cambrian Elvins Formation below to the high-velocity Carbonates above; A prominent reflector seems associated with the Bonneterre Formation Marker. This is a relatively thin and high-velocity dolomite reflector sandwiched between the lower-velocity Elvins shale above and the Lamotte Arkosic sandstone below, which makes up a high impedance contrast boundary. Nelson and Zhang (1991) suggested that the Bonneterre Formation Marker might be a regional seismic stratigraphic boundary marking the transition from active crustal extension to regional basin-wide subsidence.

Discussions

Distinct seismic phases are excited at high impedance contrast boundary between low-velocity sediments and high-velocity Paleozoic rocks; later, seismic waves are confined and reverberated within the low-velocity sediments such as P- and S-wave reverberations. For an earthquake with 7 km source depth and recorded at a station 12 km away, incidence angles for P and S waves are approximately 62º under the sediment layer and 12º and 9º within the sediment layer assuming a standard CERI velocity model. Because the thickness of sediment is relatively small in comparison to the depth of the earthquake source and the velocities of sediments are extremely low in comparison to wave velocities in the deeper regions, there are little differences in ray parameters between phases produced by the P-wave (P, PpPhp, Ps) and between phases produced by the S-wave (S, SsShs, Sp). The nomenclature for seismic phases is consistent with those in Bäth and Stefanson (1966). In the earlier numerical experiment, we found that vertical incidence two-way travel time calculation is a good approximation to the actual travel time for travel path in unconsolidated sediments. However, travel time curves for deeper reflectors deviate more from the referenced curve at zero offset as offset increases (Chiu and Langston, 2009). Thus, the relations between depths of sediment beneath stations and the corresponding two-way travel time moveouts of the reflected phases (PpPhP and SsShs) from the base of unconsolidated sediments will provide a half of velocities within the unconsolidated sediments. It gives an average velocity of 2.0 km/s and 0.7 km/s for P- and S-waves, respectively, in the upper Mississippi Embayment (Figure 10). This result agrees with those from well log data reported previously by Langston (2003a), and with those from seismic reflection profiles (Hamilton and Zoback, 1982), as well as with COCORP deep reflection survey (Nelson and Zhang, 1991) in the embayment.

The NMO migration seismic imaging profiles show a reflector correlated with low-velocity Elvins shale zone at depth about 2.8 – 3.2 km beneath GLAT, GNAR, LNXT, LPAR in the embayment as reported by Hamilton and Zoback (1982) and Mooney *e. al.*, (1983); but, no clear correlations beneath CUKY, HICK, HALT, PARM and HENM. This is consistent to the interpretations from the wide-angle reflection profile 1-5-6 at SP1 (shot point 1) in the vicinity of HICK and CUKY (Mooney *et. al*., 1983). Absence of low-velocity layer was interpreted in the cross profiles (2-3-4 and 8-5-4) at SP4 (shot point 4) near HALT in the report of the wide-angle reflection/refraction experiment (Ginzburg *et. al*., 1983). Missing low-velocity layer under PARM could be associated with the intrusion of Bloomfield pluton underneath about 2.5 km depth from the potential field study about the geophysical setting of the

Reelfoot rift and relations between rift structures and the NMSZ (Hillenbrand *et. al*., 1995). Thinner layer(s) of low-velocity zone could be underneath PEBM. More works are needed for PENM and MORT due to insufficient data to explore deeper structures (Chiu and Langston, 2009).

S-to-P and P-to-S wave conversions take place at the high impedance contrast interface between low-velocity unconsolidated sediments and high-velocity Paleozoic rocks. These converted waveforms can be used in the waveform modeling to study how shallow crustal structure responds to the incoming seismic waves. However, the very low shear wave velocity in the sediments makes transmitted Sp conversion waves always conspicuous and can be readily observed on the vertical-component. Variations of Sp wave shapes from deeper and shallow interface conversions can be clearly distinguished in the broadband waveform data. Although high- and low-frequency Sp waves should be observed at short-period seismograms, they do not appear as significantly as those shown on broadband seismograms because of the narrow bandwidth of instrument response. 'Stretching' feature of` Sp emerged in the deeper section is the nature of NMO correction due to the large incident angle in the high-velocity Paleozoic rocks while P- and S-wave paths within the sediments are near vertical incidence. Polarities of the first-motion of P- and S-wave coda as well as Sp-wave are corrected to downward motions such that interpretation of the NMO migration imaging profiles can be treated similarly to the traditional reflection seismology. Velocity models in sediments are useful in seismological study. For example, incorporating geophysical and geotechnical data, high-resolution near-surface soil structure and its high-frequency site response can be modeled using waveform inversion technique (Chiu and Langston, 2011).

Conclusions

We select events with clear P- and S-waves as well as their first reflections and transmissions from CERI local earthquake catalog. Events in all aspects of azimuth, hypocenter depth, epicenter distance, and magnitude are considered. However, events close to station are preferred to ensure simple waveform and simple propagation path to enable a better estimate of NMO corrections for reflections and transmissions in sediments. Despite very long series of high frequency near-surface site response appears on P- and S-wave, this study demonstrates that their first reflections and transmissions can be analyzed and modeled by applying pseudo-imaging profiling technique to implement NMO corrections on their displacement waveforms. Common reflectors can be identified among P-, S- and Sp-wave profiles to determine a one-layer constant velocity model for unconsolidated sediments in the ranges of 1.95 - 2.42 km/s for Vp and 0.60 – 0.73 km/s for Vs overlying a half-space of Paleozoic rocks in the ranges of 6.0 - 6.2 km/s for Vp and 3.26 – 3.6 km/s for Vs beneath seismic stations in the Mississippi Embayment. In spite of their slight variations, NMO migration imaging profiles display consistently common reflectors correlating with stratigraphic interfaces shown in petroleum exploration well logs in this region. In particular, the prominent reflectors associated with the upper Cretaceous/Holocene Mississippi Embayment Super Group, the Knox Group, and the Bonneterre Formation marker have been identified. Another strong reflector at depth of ~1 km may be associated with a dolomite layer. The top of Precambrian basement can be seen between 4.0 and 4.5 km; it seems to have a relative high impedance contrast but with little velocity contrast. A reflector is correlated with the low-velocity Elvins shale zone at depth about 2.8 – 3.2 km beneath GLAT, GNAR, LNXT, LPAR in the embayment, which was also reported by Hamilton and Zoback (1982) and Mooney *et al.*, (1983); but, no clear reflector from the imaging profiles can be identified to correlate with the low-velocity Elvins shale zone beneath stations CUKY and HICK in southwestern Kentucky, HALT in western Tennessee as well as PARM and HENM in southeastern Missouri. Similar findings were reported for profile 1-5-6 at SP1 near HICK and CUKY and for profiles 2-3-4 and 8-5-4 at SP4 close to HALT in the wide-angle refraction/reflection experiments conducted by the U.S. Geological Survey (Mooney *et. al*.1983; Ginzburg *et. al.*, 1993). The absence of clear reflector associated with the low-velocity Elvins shale zone beneath PARM may be due to the intrusion of the Bloomfield pluton at depth ~2.5 km (Hildenbrand and Hendricks, 1995).

Although slight variations of Vp and Vs in sediments, we find that travel time moveouts of reflected waves are linearly proportional to the corresponding sediment thickness beneath stations. High- and low-frequency Sp waves are observed on broadband seismograms that confirm the occurrence of multiple

wave conversions starting at deeper interfaces in the Mississippi Embayment. 'Stretching' feature of` Sp waves in the deeper section of the imaging profiling is the nature of NMO corrections due to a large incident angle in the high-velocity Paleozoic rocks while P- and S-wave paths in sediments are near-vertical incidence.

Microearthquakes do not produce large displacements; however, their waveform data can be modeled to explore wave propagation mechanisms and its implications on the earth model. The method will allow us to empirically examine site amplification of low-strain seismic waves independent of other geotechnical field experiments. These results are useful to environmental and engineering applications, as well as geological site characterization to estimate site amplification for future large strong ground motions due to significant earthquakes in the NMSZ and its proximity. The use of velocity models in the Probabilistic Seismic Hazards Assessments (PSHA) will place strong constraints on ground motion variability to address uncertainties in the PSHA estimates and can also be used to correct for site effects of attenuation in distance. These direct applications of research products will contribute to reduce losses and casualties caused by earthquakes within the plate interior. Our study reaffirms the authenticity of this technique by applying to the earthquake displacement seismograms recorded by the CUSSO borehole array; importantly, this pseudo-imaging technique using displacement seismograms of natural earthquakes is a non-invasive process.

Data and Resources

Software packages GMT (Generic Mapping Tool) (Wessel and Smith, 1998), SAC (Seismic Analysis Code) (Goldstein and Minner, 1996), and MATLAB are used widely in this study. The CNMSN seismic data were obtained from the CERI Seismic Data Archive. Data from the temporary deployment were submitted for archiving at the PASSCAL data center.

Acknowledgments

We would like to express our greatest gratitude to the anonymous reviewers for their detailed review, and valuable comments and suggestions. The Seismic Analysis Code (Goldstein Minner, 1996), and GMT (Wessel and Smith, 1998) were used for most data processing, analyses, and preparing figures and are gratefully acknowledged. This research was supported by the US Geological Survey (USGS), Department of Interior, under NEHRP grant award numbers G09AP00096 and G12AP20012, and the Center for Earthquake Research and Information, University of Memphis. We also like to thank the Institute of Earth Sciences, Academia Sinica, Taipei, Taiwan for generously providing computer facilities in order to continue this research work during my visit of Taiwan in the first-half of 2014. The views and conclusions contained in this document are those of the authors and should not be interpreted as necessarily representing the official policies, either expressed or implied, of the U.S. government.

References

Bäth M., and R. Stefansson (1966). S-P conversion at base of the crust. *Am. Geofis.*, 19, 119-130.

Bodin, P., K. Smith, S. Hortom, and J. Hwang, (2001). Microtremor observations of deep sediment resonance in metropolitan Memphis, Tennessee, *Eng. Geol*., 62, 159-168.

Catchings, R.D. (1999). Regional VP, VS, VP/VS and Poisson's ratios across earthquake source zones from Memphis, TN, to St. Louis, MO, *Bull. Seism. Soc. Am.*, 89, 1591-1605.

Chen, K.C., J.M. Chiu, and Y.T. Yang, (1996), Shear-wave velocity of the sedimentary basin in the upper Mississippi Embayment using S-to-P converted waves, *Bull. Seism. Soc. Am.*, 86(3), 848-856.

Chiu, J.M., A.C. Johnston, and Y.T. Yang, (1992). Imaging of active faults of the central New Madrid seismic zone using PANDA array data, *Seis. Res. Lett*., 63(3), 375-393.

Chiu, S.C. and C.A. Langston, (2009). Reflection and transmission imaging of the upper crust using local earthquake seismograms, *Bull. Seism. Soc. Am*., 99(5), 3039–3054.

Chiu, S.C. and C.A. Langston (2011). Waveform Inversion for Near-surface Structure in the New Madrid Seismic Zone. *Bull. Seism. Soc. Am*., 101(1), 93-108.

Chiu S.C., J.M. Chiu, C.A. Langston, Z. Wang, E. Woolery and M. Withers (2012). Shallow Crustal Velocity Structure in the Upper Mississippi Embayment Using Passive Seismic Waveforms, Present at AGU in San Francisco, CA, December, 2012.

Chiu S.C., J.M. Chiu, C.A. Langston, Z. Wang, and E Woolery (2014). Transfer Function and its Implication at the CUSSO Borehole Array in Southwestern Kentucky using Microearthquake Waveform Data, revision to be submitted to *Bull. Seism. Soc. Am*.

Cramer, C., (2006). Quantifying the uncertainty in site amplification modeling and its effects on site-specific seismic-hazard estimation in the upper Mississippi Embayment and adjacent area. *Bull. Seism. Soc. Am*., 96, 2008-2020.

Dorman, J., and R. Smalley (1994). Low-frequency seismic surface waves in the upper Mississippi Embayment, *Seis. Res. Lett.*, 65, 137-148.

Gao, F.C., (1999). High-resolution upper crustal P and S velocity structures in the upper Mississippi Embayment, MS thesis, the University of Memphis.

Ge, J. (2005). Determination of shallow shear wave velocity structure and attenuation in the Mississippi Embayment from VSP and refraction data, Master Thesis of the University of Memphis.

Ginzburg. A. W. D. Mooney, A. W. Walter, W. J. Lutter, and J. H. Healy., (1983). Deep structure of nothern Mississippi Embayment, *Am. Assoc. Petrol. Geol*. 67, 2031 – 2046.

Goldstein, P., and L. Minner, (1996). SAC2000: Seismic signal processing and analysis tools for the 21th century, *Seis. Res. Lett*., 67, 39.

Hamiltom, R., and M. Zoback (1982). Tectonic features of the New Madrid seismic zone from seismic-reflection profiles, *U.S. Geological Survey Professional Paper 1296-F*, 55pp.

Hildenbrand, T.G., and J.D. Hendricks (1995). Geophysical seting of the Reelfoot rift and relations between rift structures and the New Madrid seismic zone, *U.S.Geological Survey Professional Paper1538-E,* 30pp.

Jemberie, A.L., and C.A. Langston (2005). Site Amplification, scattering and intrinsic attenuation in the Mississippi Embayment from coda waves, *Bull. Seism. Soc. Am*, 95, 1716-1730.

Johnston, A.C. and E.S. Schweig (1996). The enigma of the New Madrid Earthquakes of 1811-1812, *Ann. Rev. Earth Planet. Sci.*, 24, pp339 – 384

Kelson, K.I., G.D. Simpson, R.B.V. Arsdale, C.C. Haraden, and W.R. Lettis, (1996). Multiple Holocene earthquakes along the Reelfoot fault, central New Madrid seismic zone, *J. Geophys. Res*., 202, 6151-6170.

Langston, C.A., (1994). An integrated study of crustal structure and regional wave propagation for southeastern Missouri. *Bull. Seism. Soc. Am.*, 84, 105-118.

Langston, C.A., (2003a). Local earthquake wave propagation through Mississippi Embayment sediments, Part I: Body wave phases and local site responses, *Bull. Seism. Soc. Am*., 93(6), 2671 – 2679.

Langston, C.A., (2003b). Local earthquake wave propagation through Mississippi Embayment sediments, Part II: Influence of local site velocity structure on Qp-Qs determination, *Bull. Seism. Soc. Am*., 93, 2685 - 2702.

Langston, C.A., P. Bodin, C. Powell, M. Withers, S. Horton, and W. Mooney, (2005). Bulk sediment Q_P and Q_S in the Mississippi Embayment, Central United States, *Bull. Seism. Soc. Am*., 95(6), 2162-2179.

Langston C.A., S. C. Chiu, Z. Lawrence, P. Bodin and S. Horton, (2009). Array observations of microseismic noise and the nature of H/V in the Mississippi Embayment, *Bull. Seism. Soc. Am*. , 99(5), 2893–2911.

Lin, T.-L., and C. A. Langston, (2009). Part I: Thunder-induced ground motions: I. Observations, *J. Geophys. Res*., 114, B042303, doi:10.1029/2008JB005769 (2009).

Lin, T.-L., and C. A. Langston (2009). Part II: Thunder-induced ground motions: II. Site characterization, *J. Geophys. Res.*, 114, B042303, doi:10.1029/2008JB005770 (2009).

Liu, H., Y. Hu, J. Dorman, T. Chang, and J. Chiu, (1997). Upper Mississippi Embayment shallow seismic velocities measured in situ, *Eng. Geol.,* 46, 313-330.

Mclntyre, J., Z.M. Wang, E. Woolery, and G. Steiner, (2011). Instrumentation and Installation of the Central United States Seismic Observatory, presented at the SSA meeting, Memphis, TN. April 13-15, 2011.

Mooney, W.D., M.C. Andrews, A. Ginzburg, D.A. Peters, and R.M. Hamilton (1983). Crustal structure of the northern Mississippi Embayment and a comparison with other continental rift zones, *Tectonophysics*, 94, 327-348.

Nafe. J. E. and C. L. Drake (1957). Variation with depth in shallow and deep water marine sediments of porosity, density, and the velocities of compressional and shear waves, *Geophysics*, 22, 523-552.

NEHRP Recommended Provision for Seismic Regulations for New Buildings and Other Structures. *FEMA-450-1/2003 Edition*.

Nelson, K.D., and J. Zhang (1991). A COCORP deep seismic reflection profile across the buried Reelfoot rift, south-central United States, *Tectonophysics*, 197, 271-293.

Rix, G.J., G.L. Hebeler, and M.C. Orozco, (2002). New-surface Vs profiling in the New Madrid Seismic Zone using surface-wave methods, *Seism. Res. Lett*., 73, 380-392.

Romero, S., and G.J. Rix, (2000). Regional variations in near surface wave velocities in the greater Memphis area. *Eng. Geol*., 61(2), 137-158.

Schneider, J.A., P.W. Mayne and G.J. Rix, (2001). Geotechnical site characterization in the greater Memphis area using cone penetration tests, *Eng. Geol*., 62, 169-184.

Stearns, R.G., (1957). Cretaceous, Paleocence, and lower Eocenc geologic history of the southern Mississippi Embayment, *Geol. Soc. Am. Bull*., 68, 1077-1100.

Street, R., E.W. Woolery, Z. Wang, and J.B. Harris, (2002). NEHRP soil classifications for estimating site-dependent seismic coefficients in the Mississippi Embayment, *Eng. Geol*., 62, 123-135.

Street, R., E.W. Woolery, and J.M. Chiu, (2004). Shear-wave velocities of the post-Paleozoic sediments across the upper Mississippi Embayment, *Seism. Res. Lett*., 75(3), 390-405.

Tuttle, M.P., and E.S. Schweig, (1999). Towards a paleoearthquake chronology for the New Madrid seismic zone, *U.S. Geol. Surv. NEHRP Ann. Rept*., 17 pp.

Tuttle, M.P., J.D. Sims, K. Dyer-Williams, I.R.H. Lafferty, and E.S. Schweig, (2000). Dating of liquefaction features in the New Madrid seismic zone, *U.S. Nuclear Commission*, 78 pp.

Van Arsdale, R.B. and R.K. TenBrink (2000). Late Cretaceous and Cenozoic Geology of the New Madrid Seismic Zone, *Bull. Seism. Soc. Am*., 90, pp345-356

Vlahovic, G., C. Powell, and J. Chiu, (2000). Three-dimensional P wave velocity structure in the New Madrid seismic zone, *J. Geophys. Res*., 105, 7999 - 8012.

Wessel, P., and W.H.F. Smith, (1998). New improved version of the Generic Mapping Tools released, Eos Trans. AGU, 79, 579.

Williams, R.A., S. Wood, W.J. Stephson, J.K. Odum, M.E. Meremonte, and R. Street (2003). Surface Seismic refraction/reflection measurement determinations of Potential Site Resonances and the Areal uniformity of NEHRP Site Class D in Memphis, Tennessee: *Earthquake Spectra*, v.19, 159-189.

Author's Affiliations, Addresses
S-C. C. C.
C. A. L.
J-M. C.
Center for Earthquake Research and Information
University of Memphis, 3904 Central Ave.
Memphis, TN 38152

Tables 1. Parameters of stations used in this study

Station	Latitude	Longitude	Elevation (m)	Description
GLAT	36.269001°	-89.288002°	120	Grass, TN
GNAR	35.965000°	-90.017998°	71	Gosnell, AR
HALT	35.910999°	-89.339996°	85	Halls, TN
HBAR	35.555000°	-90.656998°	74	Harrisburg, AR(CERI)
HENM	36.716000°	-89.472000°	88	Henderson Mound, MO
HICK	36.541000°	-89.228996°	141	Hickman, KY
LNXT	36.101002°	-89.490997°	144	Lenox, TN
LPAR	35.602001°	-90.300003°	67	Lepanto, AR
PARM	36.664001°	-89.751999°	85	Stahl Farm, MO
PEBM	36.112999°	-89.862000°	76	Pemiscot Bayou, MO
PENM	36.450001°	-89.627998°	85	Penman, Portageville, MO
MORT	36.325001°	-89.566002°	83	Mooring, TN

Table 2. Parameters of earthquakes used in the study.

Station	yyyymmdd	time	latitude	longitude	Md	depth (km)	distance (km)
GLAT	20020420	20:00:00	36.1319°	-89.3903°	2.8	6.82	17.80
	20030530	2:18:00	36.1258°	-89.3940°	2.8	6.16	18.60
	20060308	6:36:00	36.5992°	-89.5845°	2.6	10.65	45.30
	20100302	19:37:00	36.7880°	-89.3562°	3.7	8.20	57.90
	20100609	18:39:50	36.2487°	-89.4028°	2.5	5.21	10.60
GNAR	20020729	11:28:00	35.9200°	-90.0297°	2.8	8.06	5.10
	20030916	2:22:30	36.0975°	-89.7567°	2.7	6.55	27.70
	20050501	14:39:00	35.8343°	-90.1470°	2.6	9.56	18.60
	20080509	8:40:00	35.8757°	-89.9888°	2.8	11.19	10.30
	20080821	4:35:00	36.0032°	-89.8677°	2.7	11.13	14.20
HALT	20030530	2:18:00	36.1258°	-89.3940°	2.8	6.16	24.40
	20071227	1:11:10	36.1258°	-89.3940°	2.8	6.16	42.20
	20090116	21:09:30	35.6443°	-89.6913°	2.8	8.85	43.40
	20090825	6:31:50	36.2518°	-89.4340°	2.8	7.54	38.80
HENM	20091218	11:38:00	36.4507°	-89.5410°	3.1	9.06	30.10
	20100302	19:37:00	36.7880°	-89.3562°	3.7	8.20	13.00
LNXT	20031221	5:20:00	36.2883°	-89.5017°	2.7	8.77	20.80
	20060511	16:28:30	36.1602°	-89.4395°	2.1	10.00	8.00
	20060907	13:51:00	36.2715°	-89.4997°	3.3	7.56	18.90
	20070406	1:34:30	36.0903°	-89.4093°	2.7	10.62	7.50
	20091218	11:38:00	36.4507°	-89.5410°	3.1	9.06	39.00
LPAR	20040721	7:34:20	35.6905°	-90.3383°	2.0	15.36	10.40
	20070819	8:07:20	35.6815°	-90.3220°	2.1	7.14	9.10
	20090210	19:55:50	35.7490°	-90.2158°	2.0	6.14	18.00
	20090616	14:58:00	35.7260°	-90.2865°	2.1	10.78	13.80
PEBM	20020729	11:28:00	35.9200°	-90.0297°	2.8	8.06	26.20
	20031221	5:20:00	36.2883°	-89.5017°	2.7	8.77	37.80
	20071227	1:11:10	36.1245°	-89.7268°	2.8	6.43	12.00
	20080509	8:40:00	35.8757°	-89.9888°	2.8	11.19	28.70
	20080821	4:35:00	36.0032°	-89.8677°	2.7	11.13	12.20
MORT	20060907	13:51:00	36.2715°	-89.4997°	3.3	7.56	8.40
	20070203	7:46:30	36.4052°	-89.5183°	2.0	8.14	9.90

Table 3. Velocity Structures resulted from this study

Station	unconsolidated sediments			Paleozoic rocks		geological stratigraphy correlation			references
	Vp	Vs	h	Vp	Vs	unit of			
	(km/s)	(km/s)	(m)	(km/s)	(km/s)	Elvins	Super Group	Bonneterre	
CUKY	2.0	0.6	593	6.1	3.5	not clear	good	good	Chiu et. al., 2014
HICK	2.0	0.60	584	6.0	3.4	not clear	good	good	Chiu et. al., 2014
GLAT	2.0	0.70	790	6.0	3.5	clear	good	good	
GNAR	2.0	0.65	762	6.0	3.5	clear	good	good for S	
HALT	2.0	0.70	770	6.0	3.6	not clear	good	not clear	
HENM	2.1	0.65	476	6.0	3.5	not clear	good	not clear	
LNXT	2.0	0.70	816	6.0	3.4	clear	good	good	
LPAR	2.07	0.73	855	6.1	3.5	clear	good	good	
PARM	2.165	0.70	400	6.0	3.26	not clear	good	good	Chiu&Langston, 2009
PEBM	1.95	0.70	749	6.2	3.3	pos. thinner	good	good	
PENM	2.15	0.615	550	6.0	3.4	possible	good	good	Chiu&Langston, 2009
MORT	2.42	0.62	750	6.0	3.5	not clear	good	not clear	

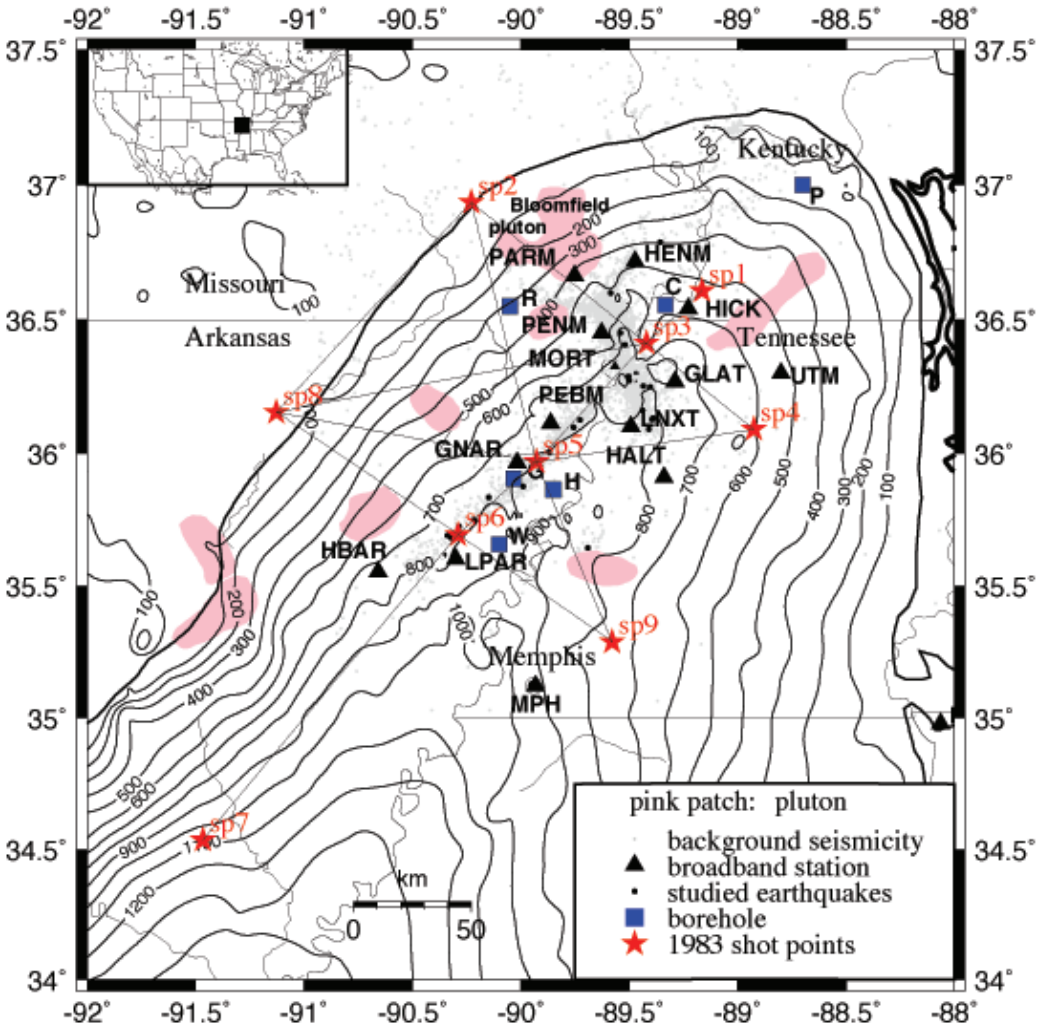

Figure 1. Location map. Solid large and small triangles are CERI broadband and short-period stations, respectively. Asterisks represent EarthScope Transportable Array stations. All are equipped with velocity sensors. Dots are the locations of earthquakes. Solid squares indicate the sites of borehole wells. Contours in intervals of 200 m show the unconsolidated sediment thickness in the Mississippi Embayment (Bodin et. al., 2001).

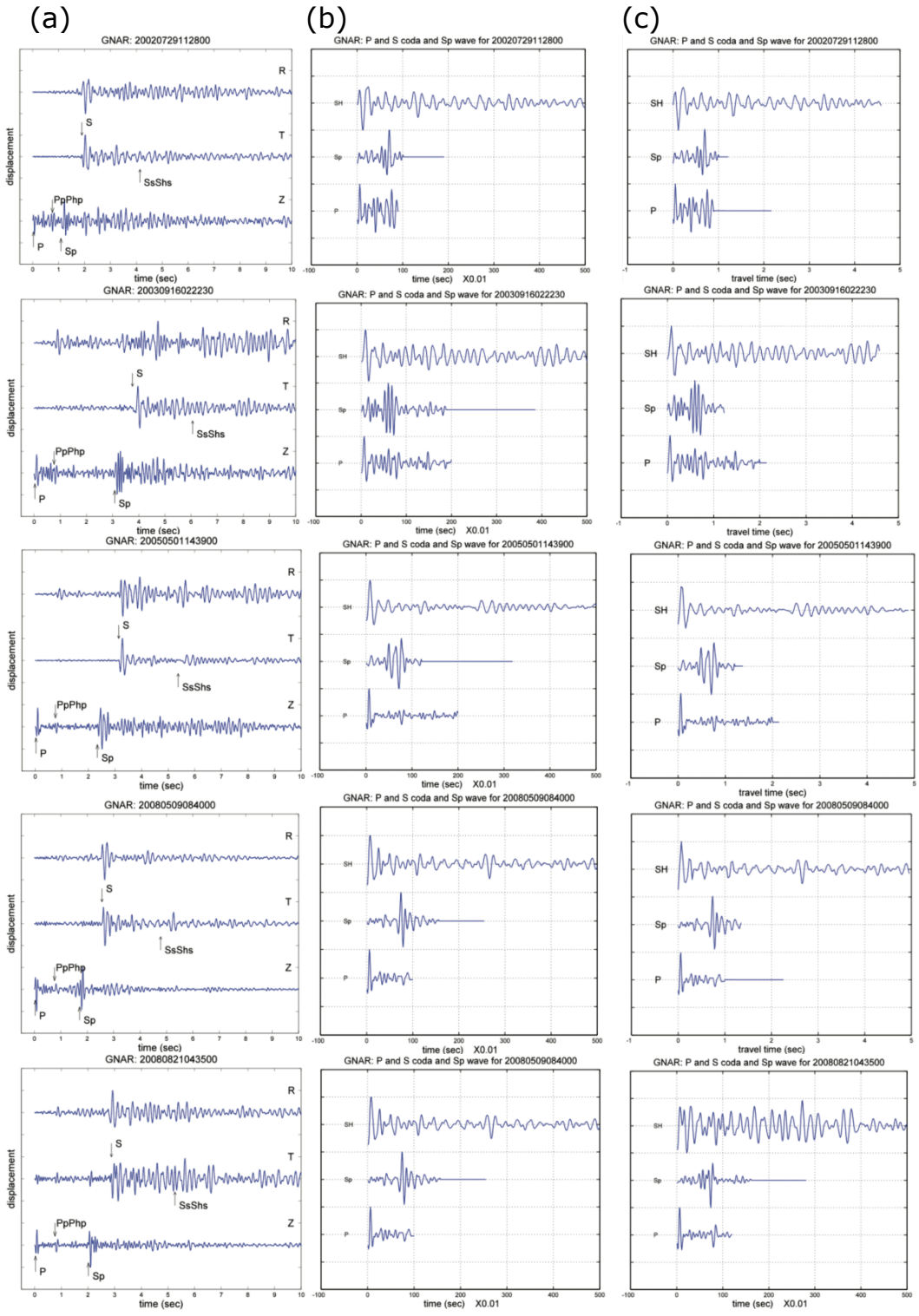
(a)
(b)
(c)
GNAR: 20020729112800
GNAR: P and S coda and Sp wave for 20020729112800
GNAR: 20030916022230
GNAR: P and S coda and Sp wave for 20030916022230
GNAR: 20050501143900
GNAR: P and S coda and Sp wave for 20050501143900
GNAR: 20080509084000
GNAR: P and S coda and Sp wave for 20080509084000
GNAR: 20080821043500
GNAR: P and S coda and Sp wave for 20080509084000
GNAR: P and S coda and Sp wave for 20080821043500
displacement
time (sec)
time (sec) X0.01
travel time (sec)
R
T
Z
S
SsShs
PpPhp
P
Sp
SH

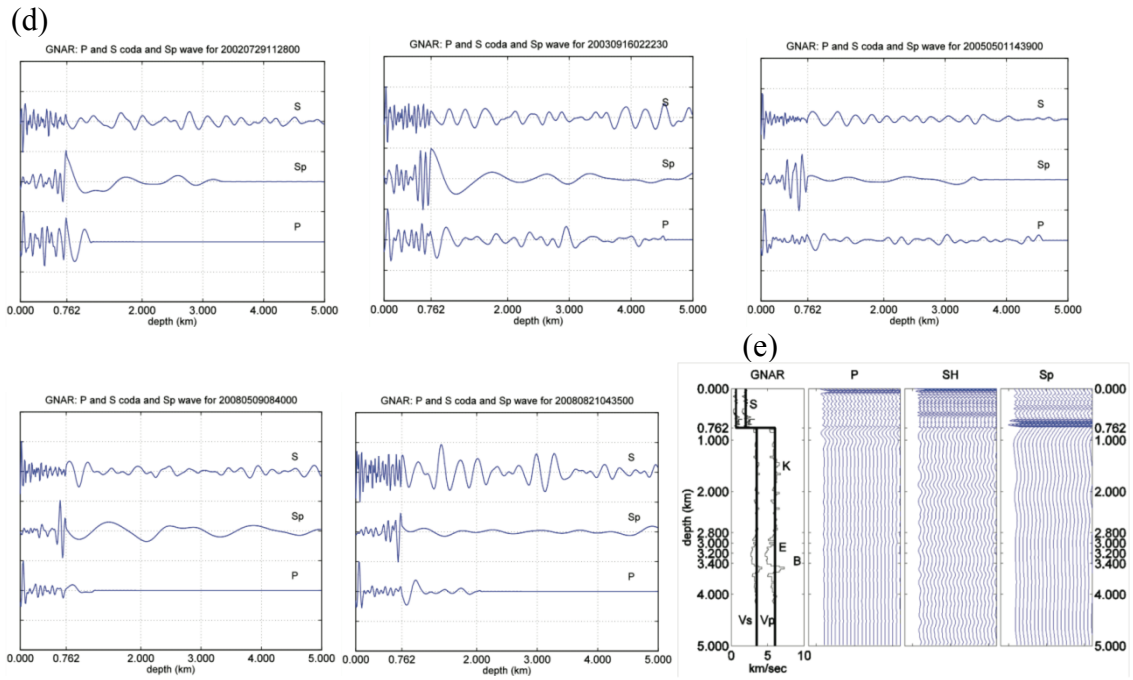

Figure 2. GNAR imaging profiling. (a) Microearthquake displacement waveforms used at GNAR. Station is equipped with velocity sensor. Ground motion is sampled at 100 samples/s. Major seismic phases are annotated. (b) P wave coda from vertical-component (Z) (back to Sp phase) and S wave coda from T-component seismograms. Sp waves are taken from the Z-component seismograms in a window after P-wave coda to the time of the peak of SV-wave arrival on R-component and then reverse in time. Sp waveforms with peak of SV arrival as zero reference time. (c) NMO corrected waveforms with peak arrivals at zero reference time in a function of two-way travel time for P- and S- wave coda and one-way travel time for Sp-wave, extending to a depth of 5 km. Interestingly, SV converted to P from interfaces at various depths occur within a few tenths of seconds. (d) Migrated P-, S- and Sp-waveforms in a function of depth. All waveforms are normalized to their individual maximum amplitude within actual time or depth window for Figure (a)–(d). Polarities of peak of P-, S- and S -wave are corrected to negative. (e) Pre-stacking NMO migrated imaging profiling constructed using a constant velocity layer of Vp 2.0 km/s and Vs 0.65 km/s overlying a half space of Vp 6.0 km/s and Vs 3.5 km/s (thick lines). Detailed velocity model is included and indicated as thin lines. Depth scale is same in four panels. Common reflectors are indicated by tick marks. A strong reflector seems to correlate consistently to the interface at depth of 762 m among all wave types. P-wave imaging profile does not seem to have enough information because of a shorter P-S time (less than 3 s). Reflectors seem to correlate well to Elvins shale zone and Bonneterree Formation in S imaging profile. S: Mississippi Embayment Super Group; K: Knox Group; E: Elvins shale; B: Bonneterre Formation Marker.

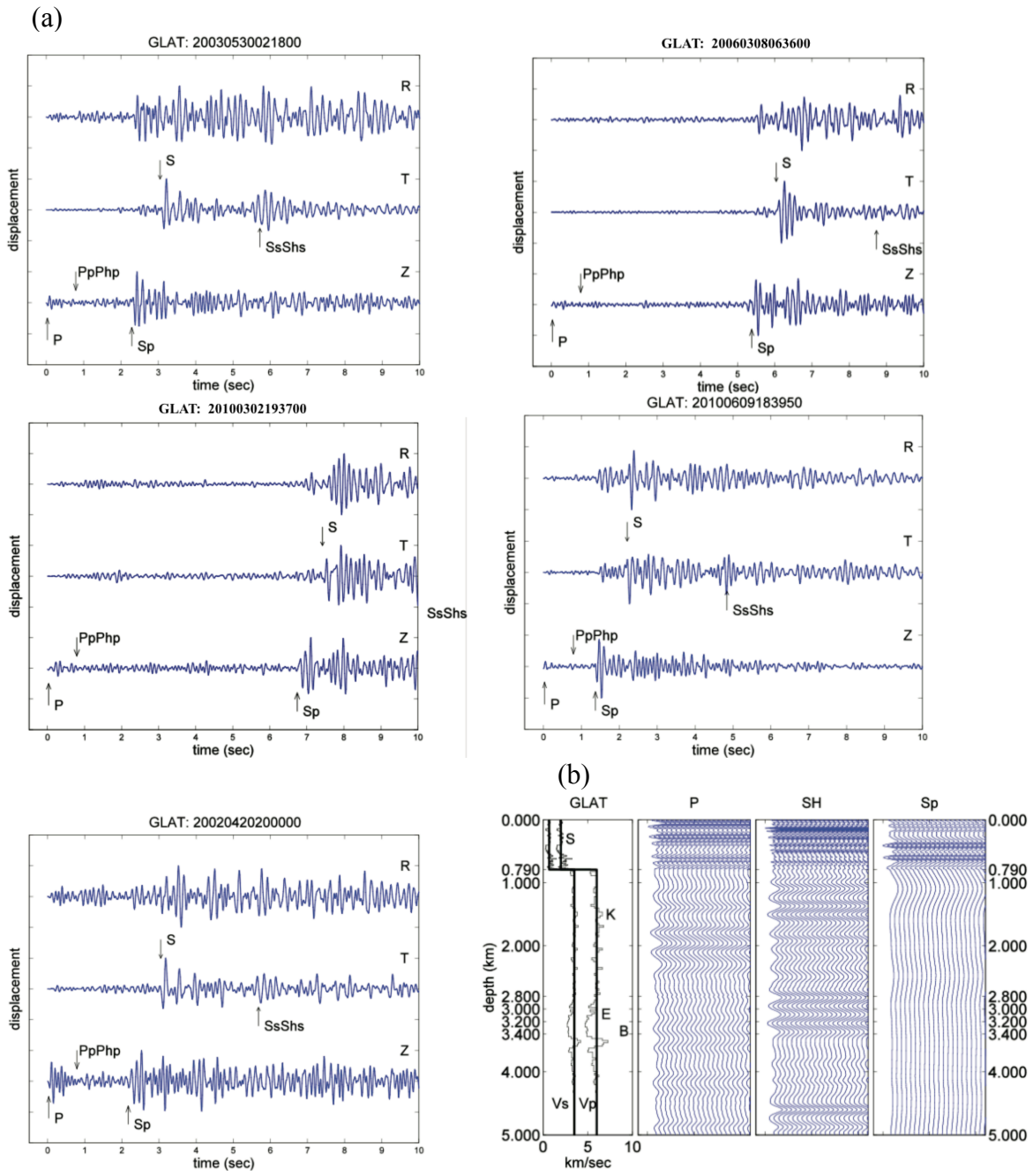

Figure 3. GLAT imaging profiling. (a) Microearthquake displacement waveforms used at GLAT (same format as Figure 2a). (b) Pre-stacking NMO migrated imaging profiling (same format as Figure 2e) computed by using a constant velocity layer of Vp 2.0 km/s and Vs 0.7 km/s overlying a half space of Vp 6.0 km/s and Vs 3.5 km/s. Consistently common reflectors appear associated with the base of Super Group at depth 790 m, carbonate layer at 1 km depth, low-velocity Elvins shale at 3.2 km and high-velocity Bonneterre Formation at 3.4 km depth.

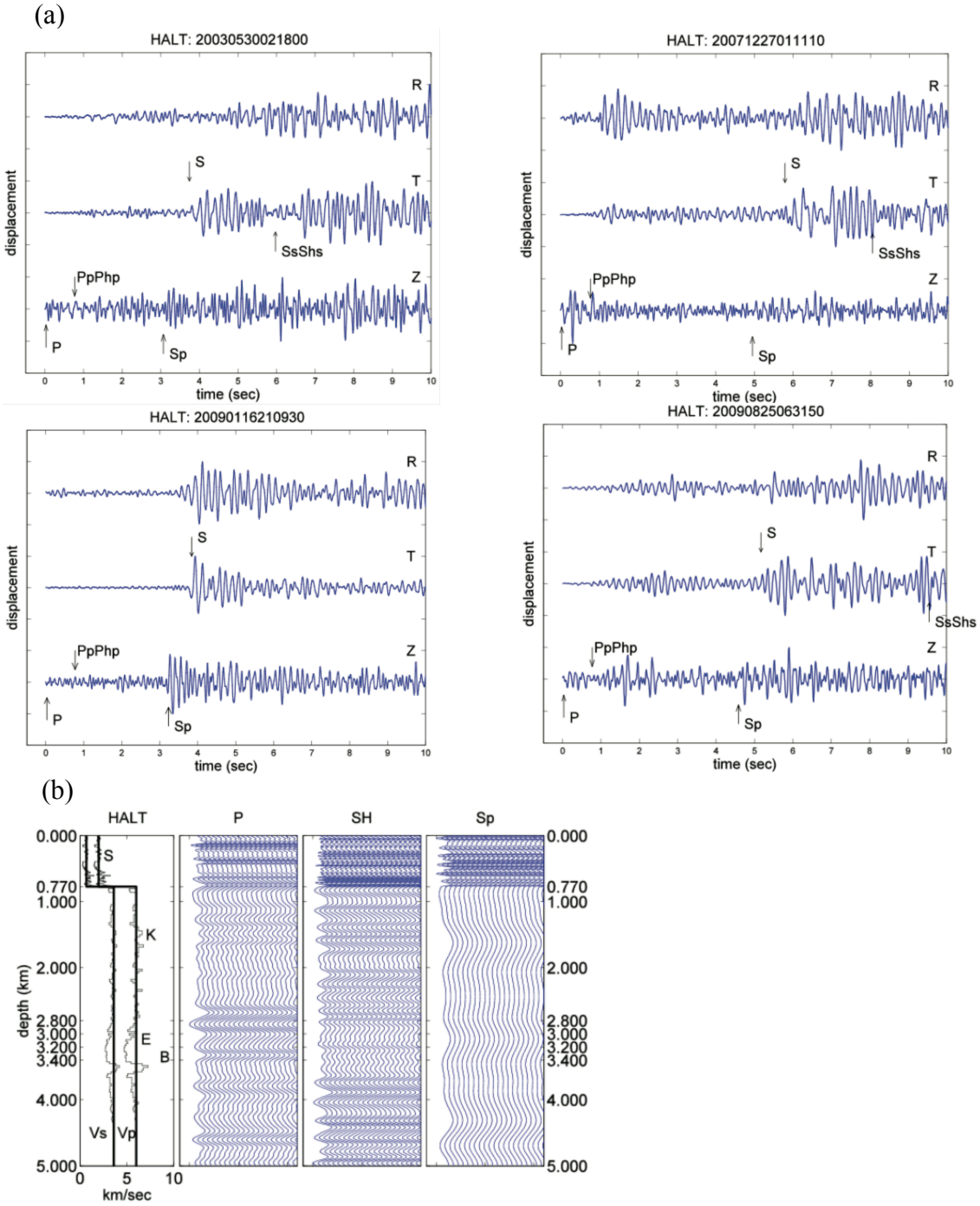

Figure 4. HALT imaging profiling. (a) Microearthquake displacement waveforms used at HALT (same format as Figure 2a). (b) Pre-stacking NMO migrated imaging profiling (same format as Figure 2e) computed by using a constant velocity layer of Vp 2.0 km/s and Vs 0.7 km/s overlying a half space of Vp 6.0 km/s and Vs 3.6 km/s. A strong reflector appears to associate with the base of Super Group at 770 m among all wave types.

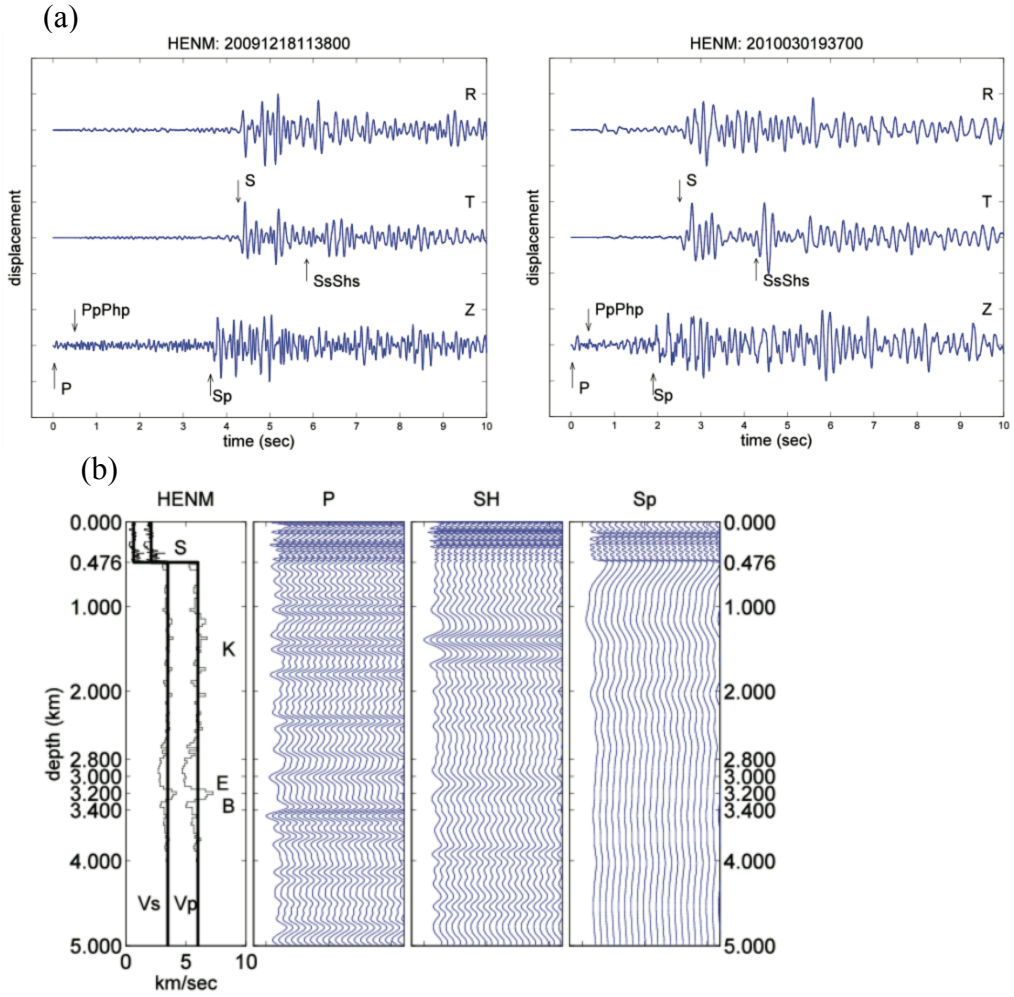

Figure 5. HENM imaging profiling. (a) Microearthquake displacement waveforms used at HENM (same format as Figure 2a). (b) Pre-stacking NMO migrated imaging profiling (same format as Figure 2e) constructed using a constant velocity layer of Vp 2.1 km/s and Vs 0.65 km/s overlying a half space of Vp 6.0 km/s and Vs 3.5 km/s. It reveals a strong reflector at depth 476 m that can be associated with the Mississippi Embayment Super Group.

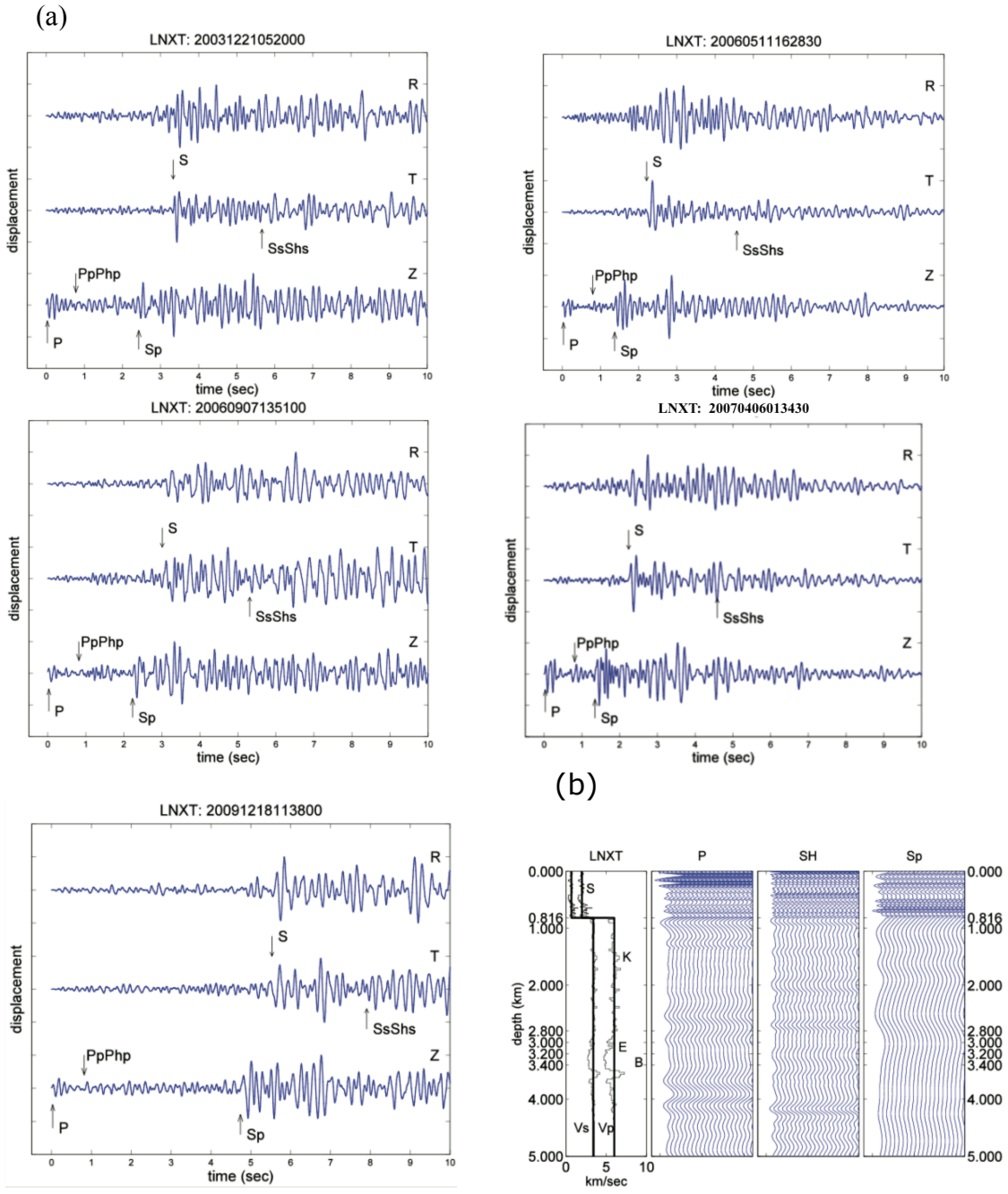

Figure 6. LNXT imaging profiling. (a) Microearthquake displacement waveforms used at LNXT (same format as Figure 2a). (b) Pre-stacking NMO migrated imaging profiling (same format as Figure 2e) computed using a constant velocity layer of Vp 2.0 km/s and Vs 0.7 km/s overlying a half space of Vp 6.0 km/s and Vs 3.4 km/s. It shows strong reflectors that can be associated with the Mississippi Embayment Super Group at 816 m depth and high-velocity Bonneterree Formation Marker. A reflector seems to associate with the low-velocity Elvins shale layer.

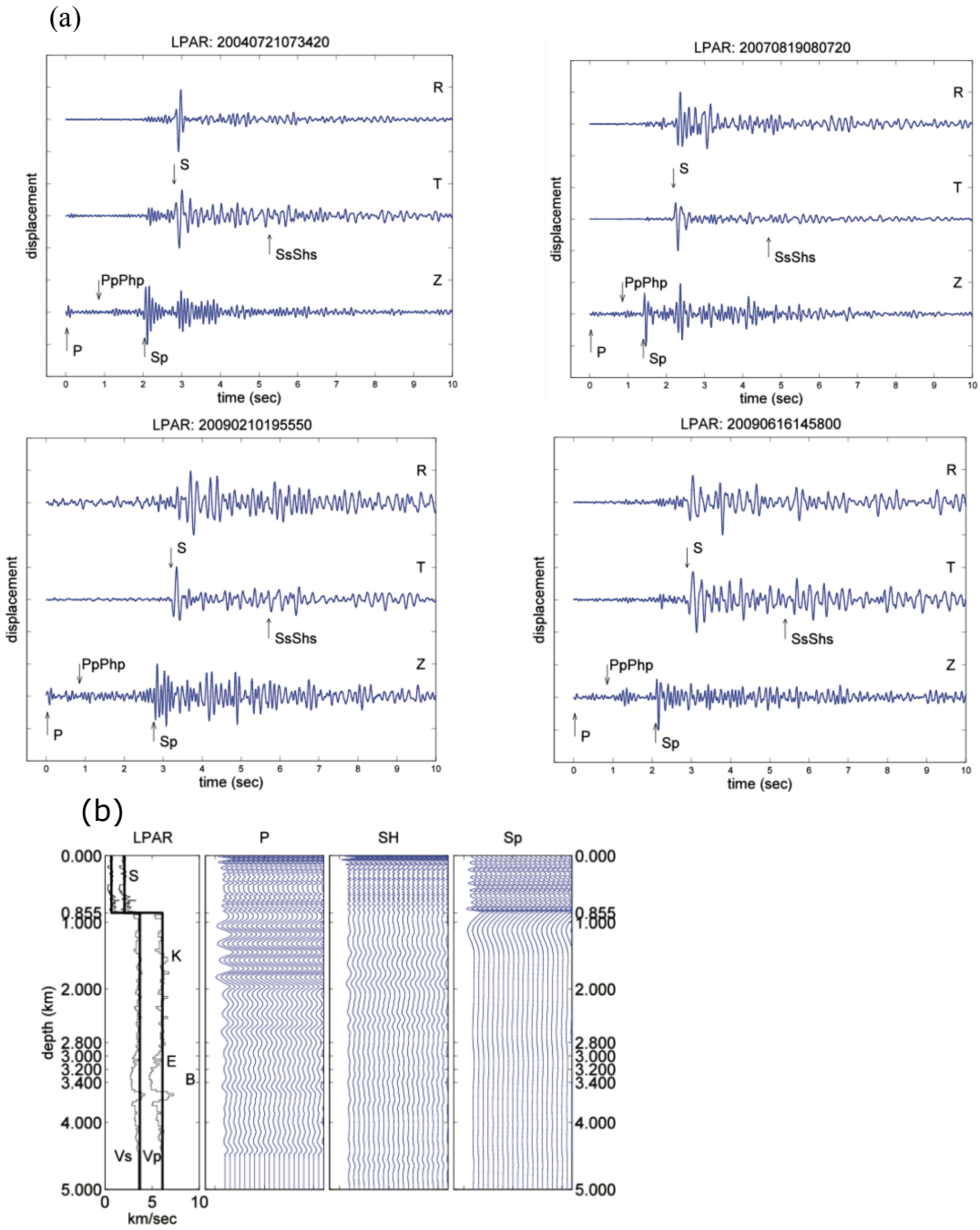

Figure 7. LPAR imaging profiling. (a) Microearthquake displacement waveforms used at LPAR (same format as Figure 2a). (b) Pre-stacking NMO migrated imaging profiling (same format as Figure 2e) computed using a constant velocity layer of Vp 2.07 km/s and Vs 0.73 km/s overlying a half space of Vp 6.1 km/s and Vs 3.5 km/s. It shows strong reflectors that can be associated with the Mississippi Embayment Super Group at 855 m depth and high-velocity Bonneterree Formation. A reflector seems to associate with the low-velocity Elvins shale layer.

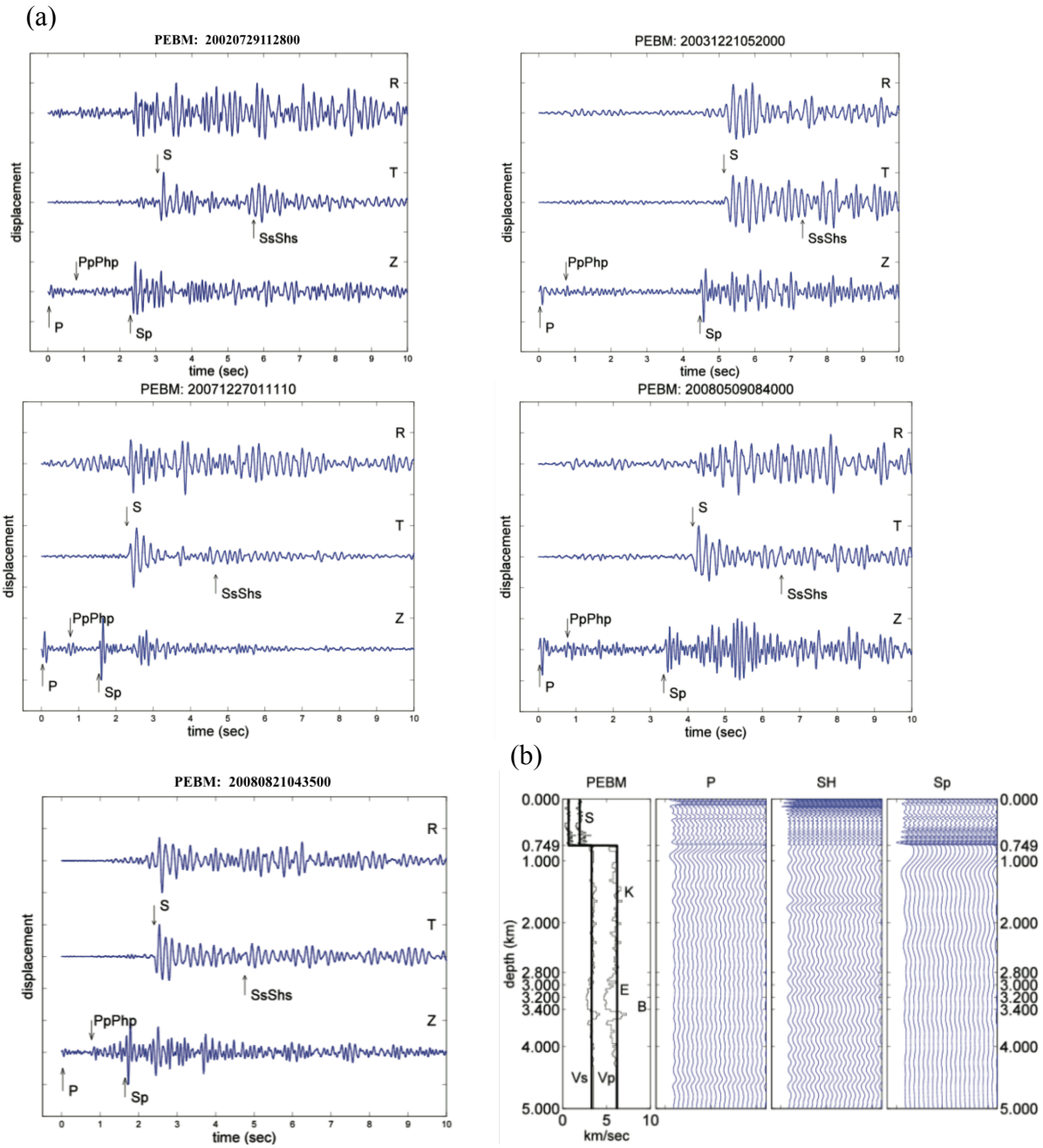

Figure 8. PEBM imaging profiling. (a) Microearthquake displacement waveforms used at PEBM (same format as Figure 2a). (b) Pre-stacking NMO migrated imaging profiling (same format as Figure 2e) computed using a constant velocity layer of Vp 1.95 km/s and Vs 0.70 km/s overlying a half space of Vp 6.2 km/s and Vs 3.3 km/s. It shows a strong reflector that can be associated with the Mississippi Embayment Super Group at 749 m depth among all wave types. Two reflectors seem to associate with the low-velocity Elvins shale layer and high-velocity Bonneterree Formation between P- and S-wave.

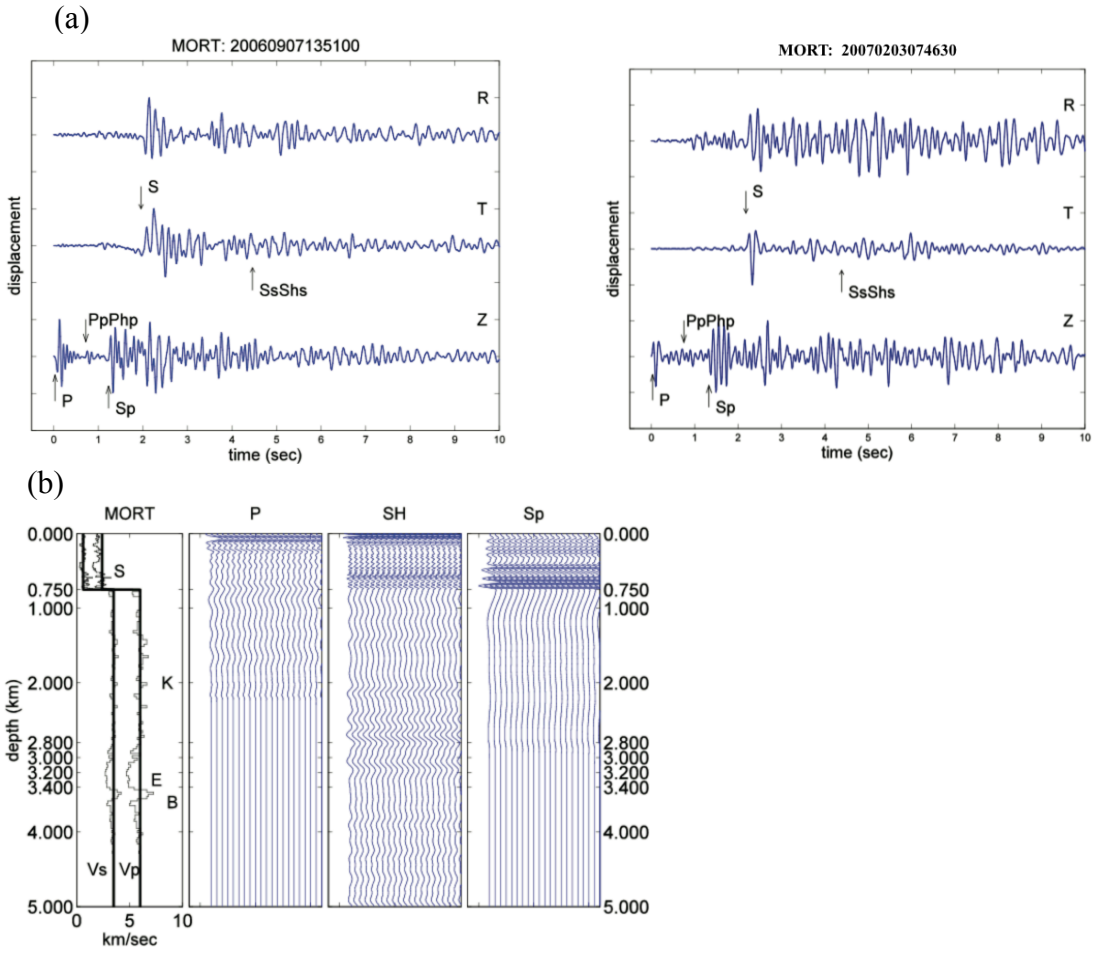

Figure 9. MORT imaging profiling. (a) Microearthquake displacement waveforms used at MORT (same format as Figure 2a). (b) Pre-stacking NMO migrated imaging profiling (same format as Figure 2e) computed using a constant velocity layer of Vp 2.42 km/s and Vs 0.62 km/s overlying a half space of Vp 6.0 km/s and Vs 3.5 km/s. The imaging emerges a prominent reflector that can be associated with the Mississippi Embayment Super Group at 750 m depth. It appears that there is a lack of rich frequency content in the short-period seismograms due to the narrow bandwidth in the instrumentation response.

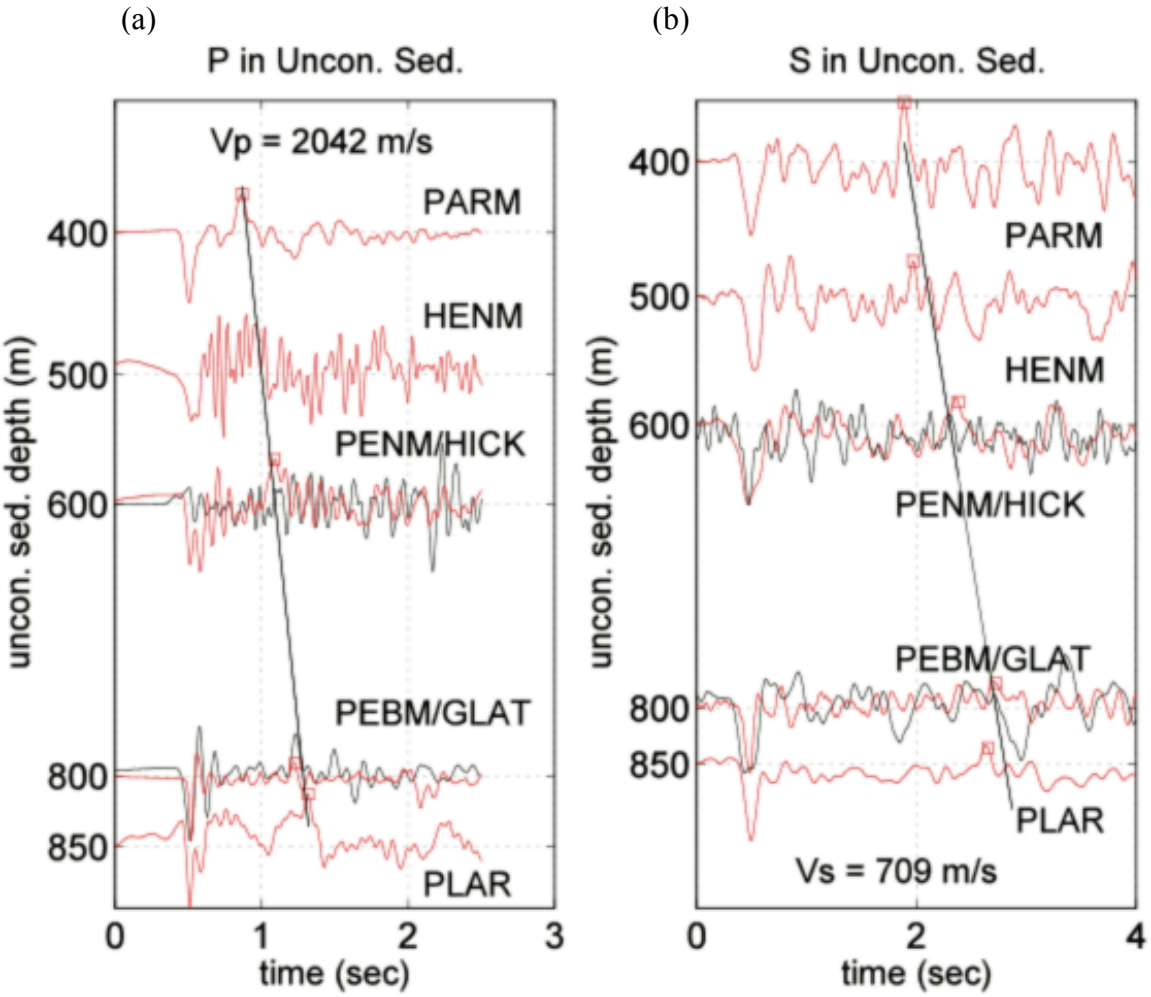

Figure 10. First-order velocity in the sediments using travel time moveouts of P- and S-wave reflections with respect to sediment depth. Squares indicate the arrivals of reflections (PpPhp or SsShs), respectively. 2.042 km/s for P-wave (a) and 0.709 km/s for S-wave (b) represent a velocity model for the unconsolidated sediments within the NMSZ. Station names are annotated.

Attachment 2

Transfer Function and its Implications at the CUSSO Borehole Array in Southwestern Kentucky using Microearthquake Waveform Data

Shu-Chioung Chi Chiu[1], Jer-Ming Chiu[1], Charles A. Langston[1], Zhenming Wang[2], and Edward Woolery[2]

[1]CERI, The University of Memphis, Memphis, TN 38152

[2]Dept. of Earth & Environmental Sciences, University of Kentucky, Lexington, KY, 40506

Abstract

We take advantage of 1-D pseudo-imaging technique using P- and S-wave coda including their reflected waves and transmitted Sp-wave shown on local earthquake displacement waveforms on stations, HICK and CUKY, in an attempt to identify common reflectors and to resolve a velocity model for deep unconsolidated sediments in southwestern Kentucky. Normal moveout (NMO) migrated seismic depth sections reveal prominent reflectors that can be correlated with subsurface interfaces at Mississippi Embayment Super Group and high-velocity Bonneterre Formation Marker; yet, there doesn't appear to have a reflector associated with the low-velocity Elvins shale interface. Consequently, a one-layer constant velocity model of Vp 2.0 km/s and Vs 0.6 km/s can be used to represent the structure for the entire unconsolidated sediments column. This result is consistent with waveform observations from P- and S-wave at the surface and base of sediments as well as S-Sp differential travel time at surface recordings in the borehole array of Central US Seismological Observatory (CUSSO). This leads to a Vp/Vs 3.3 and Poisson's ratio 0.5. However, Vs of 0.6 km/s is higher than ~0.4 km/s from the direct measurements at the CUSSO logging site, suggesting that the accuracy of the CUSSO logging data may need to be re-evaluated.

Transfer function of unconsolidated sediment system is computed by de-convolution of a local earthquake displacement spectrum at the surface to the base of the CUSSO array in the upper Mississippi Embayment. The NMO migration seismic sections for the transfer function time series are calculated by using the one-layer constant velocity model for unconsolidated sediments mentioned earlier overlying a half-space of Paleozoic rocks with Vp 6.0 km/s and Vs 3.4 km/s. A clear near-surface reflector at depth ~10 m is associated with a thin zone of weathering soils. Modulus of the transfer function indicates that ground motion is amplified more than 10 times at a frequency ~20 Hz for P-wave, which can be correlated with the nearly-vertical incident P-wave reverberated at a period 0.05 s in the low-velocity near-surface soils. This information provides a useful indicator of the dominant frequency of vibration at which the most significant ground motion effects of amplifying and prolonging shaking duration can be expected during a future large earthquake. Therefore, the frequency-dependent site responses of loose sediments should be of great concerns for the environmental engineering and the earthquake hazard assessment to reduce economic losses and protect communities in the central and eastern US. In addition, this study in using vertical array data reaffirms the authenticity of the 1-D pseudo-imaging profiling technique.

Introduction

The New Madrid Seismic Zone (NMSZ) is the most seismically active region in the United States east of the Rocky Mountains (Figure 1). Since late 1974, more than 10,000 earthquakes were recorded instrumentally and archived at the Center for Earthquake Research and Information (CERI), University of Memphis. Evidences of widely distributed liquefaction from previous paleoseismological studies and a relatively concentrated and active local earthquake seismicity reveal strongly the potential of future damaging earthquakes in the NMSZ. The Mississippi Embayment, overlying much of the NMSZ, is filled with thick Cretaceous to present sediments about 1 km thickness at the latitude of Memphis, Tennessee (Stearns, 1957; Figure 1). Categorized by averaging shear wave velocity in the top 30 m of loose soils, i.e. Vs30, site conditions of the embayment are classified as either D (Vs of 180 m/s to 360 m/s) or E (Vs < 180 m/s) (FEMA-450-1, 2003) in the National Earthquake Hazards Reduction Program (NEHRP). The sediments in the embayment are characterized by an extremely low shear wave velocity and large impedance contrast between the unconsolidated sediments and the underlying Paleozoic bedrock. As a consequence, the structural environment has a significant impact on earthquake ground motions by amplifying and prolonging the shaking due to a large earthquake. In the past, ground motions of the loose Ohio River deposits caused approximate $3 million damages in Maysville, Kentucky, by the magnitude 5.2, Sharpsburg, Kentucky, earthquake in 1980. Examples of displacement seismograms are plotted in Figure 2 showing ground motions recorded by sensors located on the bedrocks and at the surface of the CUSSO borehole array for a magnitude 4.7 earthquake occurred February 28, 2011 near Greenbrier, central Arkansas, and the magnitude 9.0 Japan earthquake occurred on March 11, 2011 (Mclntyre *et. al.,* 2011). It demonstrates that ground motions were largely amplified at various levels for different frequencies and waveforms became much more complicated after propagating from the top of Paleozoic basement to the ground surface. The frequency-dependent site amplification is apparently due to the existence of loose, thick, and complex sediments in the Mississippi Embayment. The scale of amplification relates not only to earthquake magnitude but also depends substantially on the transfer function of the entire sediment column as well as the seismic attenuation along the propagating path. Communities such as Memphis, Tennessee, St. Louis, Missouri, and Paducah, Kentucky in the central United States are built on the top of soft soils along the Mississippi and Ohio Rivers. Site responses in the upper Mississippi Embayment should be a primary interest concerning earthquake hazard assessment in the central and eastern US. In other parts of the world, the characteristics of ground motions caused by great earthquakes are significantly affected by the local site conditions, e.g. 1985 Mexico, 1988 Armenia, 1989 Loma Prieta, 1994 Northridge, 1999 Chi-Chi, Taiwan, and 2001 Gujurat, India, earthquakes. These observations highlight the urgent need of understanding site response induced by soft sediments and its potential impacts from future large earthquake in the NMSZ.

Site classifications and Vs30 information (Williams *et. al.,* 2003) have been adopted by the NEHRP standard (FEMA-450-1, 2003) to estimate site amplification and to predict strong ground motions for seismic hazard maps as done in the Memphis area (Cramer*,* 2006), and Seattle, Washington (Williams *et. al.,* 1997). Recent geotechnical field experiments such as Vertical Seismic Profiling (VSP; Liu *et. al*., 1997) and Seismic Cone Penetration Tests (SCPT; Schneider *et. al*., 2001) showed that Vs profiles have little variations in the upper 30+ m (Liu *et. al.,* 1997; Rix *et. al.,* 2002) while Vp increases rapidly down to the water table ~10 m and retains an average of 1.8 to 2.0 km/s below (Liu *et. al.,* 1997). Yet, geotechnical data or a simple Vs30 model may not properly predict site responses nor yield wave propagation effects due to the averaging used over the extremely complicated structure.

Due to the high impedance contrast between the low-velocity unconsolidated sediments above and high-velocity Paleozoic rocks below, the up-going P (S) wave from earthquake is reflected at the free surface and is subsequently trapped and reverberated inside the unconsolidated embayment sediments. Similarly, the P (*S*) wave can resonate in the extremely low-velocity near-surface soils overlying the unconsolidated sediments. Figure 3 is an example of displacement seismograms of a local earthquake showing four major features: the direct primary P- and S-wave (P and S), the identifiable P and S reflected waves (PpPhp and SsShs), S converted P wave at the bottom of the unconsolidated sediments (Sp), and the resonances in the near-surface soft soils (nP and nS). The nomenclature for seismic phases

is consistent with those in Bäth and Stefanson (1966). In this study, we utilize 1-D pseudo-imaging profiling technique to implement NMO corrections on the reflected P- and S-wave and converted Sp-wave such that reflection and transmission effects are contributed to the common reflectors. Incorporating near-by well logging data, the imaging profiling can be interpreted similarly to the traditional reflection seismology. Details about this technique can be found in Chiu and Langston (2009) and is briefly summarized in the following sections.

Velocity Structure in the Mississippi Embayment

The northern Mississippi Embayment is filled with thick unconsolidated sediments consisting mostly clastic sediments associated with the Mississippi River and glacial loess deposits ranging in age from upper Cretaceous to recent. The geological character of the embayment is not significantly different from other areas along the coastal plains of the southeastern United States that are covered mostly by the coastal unconsolidated sediments. Average velocity models for the large- and relatively small-scale geological structure associated with Reelfoot Rift Zone have been studied by many investigators, e.g. wide-angle seismic refraction/reflection experiments (Mooney *et. al*., 1983; Ginzburg *et. al.,* 1983; Catchings, 1999; Nelson and Zhang, 1991; Langston *et. al.,* 2005), tomographic studies of travel times (Gao, 1999; Vlahovic *et. al.,* 2000), surface wave dispersion study (Dorman and Smalley, 1994), and Vertical Seismic Profiling (VSP) (Liu *et. al.,* 1997). Other studies used local earthquake waveforms to explore average P- and S-wave velocities and site responses for the unconsolidated sediments (e.g. Chen *et. al.,* 1996; Bodin *et. al.,* 2001; Chiu and Langston, 2009; Chiu *et. al.,* 2011), as well as waveform inversion modeling (Langston, 2003; Chiu and Langston, 2011).

In addition to P-wave velocity, S-wave velocity and density are the required parameters for computations in the 1-D pseudo-imaging method. However, deep acoustic well logs in this region are distributed sparsely; meanwhile, there are currently no extensive loggings in this region for either S-wave velocity or bulk density. Dorman and Smalley (1994) suggested an empirical approach for deriving both parameters from exploration of acoustic well log data using a Nafe-Drake type sediment model (Nafe and Drake, 1957) as shown in equations (1) and (2).

$$\rho = (1-\phi)\rho_S + \phi\rho_W$$

$$V_P^2 = \frac{\rho_S}{\rho}(1-\phi)^5 V_{Ps}^2 + \phi(1+\frac{\rho_W}{\rho}(1-\phi))V_{Pw} \qquad (1)$$

$$V_S^2 = (1-\phi)^n V_{Ss}^2 \qquad (2)$$

where Porosity (φ) is derived from the observed P-wave velocity (V_p), an assumed solid model P-wave velocity (V_{Ps} 6.1 km/s), water P-wave velocity (V_{Pw} 1.5 km/s), solid model density (ρ_s 2.7 g/cm^3), and water density (ρ_w 1 g/cm^3); S-wave velocity (Vs) is derived from an assumed solid model S-wave velocity ($V_{Ss,}$ 3.5 km/s) and resulting porosity (φ) with exponential power of 5.6 as suggested by Langston (2003).

In 2008, a deep borehole array has been installed by the University of Kentucky at the CUSSO well site, located at 36.5540°N, 89.3320°W. Direct measurements of logging data at this well starting at depth 2.6 m down to 593 m with an average interval of 0.5 m. Therefore, P- and S-wave data are available for a total of 637 sampling points. Figure 4 shows a collection of velocity models, density, Vp/Vs ratio and porosity for four well logs consisting of CUSSO, Garigan (G), Haynes (H), and Wilson 2-14 (W). Their locations are shown in Figure 1. Each well log data is presented by 100 layers. P wave slowness in each layer is determined by averaging slowness over a depth range by preserving vertical travel time. Velocity is the reciprocal of averaging slownesses. S-wave velocity is derived from the acoustic log data assuming Nafe-Drake sediments model except direct measurements for the CUSSO deep borehole. P-wave velocity appears considerable heterogeneity with depth but has an average of 1.8-2.0 km/s below water table. Its variability in the CUSSO well log is similar to others; though, borehole Vs profile from direct measurements appears about half slower down to ~ 0.3 km. In contrast to an average S-wave velocity of

0.6 - 0.7 km/s in the NMSZ, an average S-wave velocity of ~0.4 km/s is obtained for the measured CUSSO borehole logging data. This contradicts to the waveform observations at the CUSSO borehole array (Figure 5). In this manner, we are not certain about the credibility of drilling measurements for S-wave.

Many acoustic well log data from oil exploration are available for other studies in this region previously. Perhaps, the most reliable and detailed data is well log at the Wilson 2-14 taken in February 2001, near Kaiser, Arkansas. Because the physical properties of unconsolidated sediments in the region do not dramatically vary as a function of depth, we assume that the acoustic well log data of the Wilson 2-14 can be used and scaled to depth of sediments beneath each station. In the meantime, S-wave velocity can be derived using an empirical approach. We also assume that the acoustic well log data of the Dow Chemical/Wilson #1 can represent Paleozoic rocks assuming Poisson's solid throughout the entire basin. An average Vp of 6.0 km/s and Vs of 3.5 km/s are found from Dow Chemical/Wilson #1 well log data. Accordingly, we construct a thin-layered earth model consisting of detailed acoustic variations in the Phanerozoic sediments down to depth of ~4 km. We refer it as the detailed velocity model in this research project. Nonetheless, the Wilson 2-14 well model might not be the best to represent velocity structure beneath station; and/or laterally heterogeneous structure might exist in close distances. Paleozoic sedimentary rocks may or may not be Poisson's solid. Two velocity models are considered here. One is the detailed model. The other model is constructed by smoothing and simplifying P- and S-wave velocity structures to facilitate the calculation of travel time curves and synthetic seismograms. High frequency scattering effects are smoothed by using a causal Butterworth bandpass filter with corner frequencies of 0.5 and 5 Hz for P- and Sp-wave and of 0.5 and 10 Hz for S-wave such that all waves exhibit similar frequency waveforms. We will also allow small adjustments to Vp and Vs in the NMO migration process to determine a velocity model so that reflection and transmission effects can be attributed to common reflectors among P-, S-, and Sp-waves.

Microearthquake waveforms recorded by the CUSSO borehole array

A Md 3.1 earthquake occurred on December 18, 2009 @11:38:08.66 UTC located at 36.451˚N, 89.541˚W, east of Point Pleasant, MO. was recorded by the CUSSO borehole array. Its radial-, transverse-, and vertical-component displacement seismograms from the surface and the base stations are shown in Figure 5. Major seismic phases are annotated. It confirms that multiple converted Sp waves, starting from deeper interfaces, are visible on both vertical-component seismograms (Z). The relatively high-frequency Sp waves are converted at shallower depths across the high impedance contrast boundary between unconsolidated sediments and Paleozoic basement rocks. Evidently, low-frequency Sp-wave is not as prominent as the high-frequency Sp-wave and is apparently converted at interfaces deeper than the top of Paleozoic basement. The horizontal-component data - sh1a (N-S) and sh2a (E-W) of surface station are rotated into the theoretical radial- direction (Urs) and transverse-direction (Uts) to facilitate the separation of P and SV motions from SH motions. Due to the nature of the equivocal orientations of the two horizontal components in the deep borehole sensor, comparison of its S-wave particle motions (Figure 6) between the surface and depth sensors suggests that bh1v, apparently, is oriented in the radial-direction and bh2v is in the transverse-direction. In addition, amplitude of the S-wave particle motions increases and seems to experience more scattering as waves propagate through the sediments. Based on the sediment depth as well as the differential travel times between the top and the bottom receivers, average velocities for the entire column of unconsolidated sediments in the borehole array are obtained as 2.0 km/s and 0.6 km/s for P- and S- wave, respectively. Given these velocities and sediment thickness, it confirms the observed time separation between direct S- and converted Sp-wave on the surface vertical-component (Z) (Figure 5). In addition, S-wave velocity is similar to the derived average values from the other three well logging data as shown in Figure 4a and is also consistent to the previous studies in this region. These results imply a Vp/Vs ratio of 3.3 and a Poisson ratio of 0.5. As a consequence, we cast doubts about accuracy of the direct measurements in the CUSSO well logging data.

Hypothesis

The hypothesis of this research is that microearthquake displacement waveform can provide an accurate view of wave propagation mechanism. A corollary of this hypothesis is that both earthquake waveforms and geotechnical data can be jointly modeled to produce a much more reliable model of earth structure and to predict the wave propagation effect.

Methodology: Pseudo-imaging Profiling Technique

This method capitalizes on the facts that the unconsolidated sediments have very low velocities and relatively high Q (Qp 500, Qs 250) with respect to the underlying Paleozoic sedimentary rocks so that the first reverberations of P and S (PpPhp and SsShs) waves can be observed and identified from the displacement seismograms. Observed arrival times for primary and reflections of the P- and S-wave, and transmission Sp-wave will place strong constraints on identifying the common reflector and determining the velocity model. This study aims to explore the ground responses of deep and shallow sediments due to natural earthquake shakings and to determine a representative velocity model beneath the station within the sedimentary basin in southwestern Kentucky. Data processes involved in analyzing ground motions of local earthquakes used in this technique include: (1) selection of microearthquakes with clear P-, S-, and Sp-phases; (2) correction of DC offset and trend, changing all times with respect to origin time, removing instrument response, integrating to displacement, and rotating along the great circle; (3) extraction coda of P-, SH-wave, and Sp-wave; (4) correction of referenced phase polarity to negative first motion; (5) correlation of waveforms to determine time shift and choosing the zero-time reference; (6) shifting all waveforms to the zero reference time at peak of the first pulse; (7) stacking; (8) performing NMO migration; (9) imaging profiling; and (10) interpretation.

There are four steps involved in the imaging process: (1) construction of an appropriate crustal velocity model; (2) calculation of two-way travel times for P- and S-wave and one-way differential travel times between P- and S-wave for Sp-wave using average interval velocities and actual ray parameter; (3) using a "stretching" operator to convert seismic time series to a function of depth to implement the NMO correction and construct a depth migration seismic section; and (4) identification and correlation reflectors to known geological interfaces from nearby well log. Thus, interpretations of 1-D seismic migration depth section can be made in a similar way to the interpretation of the traditional seismic reflection profile. NMO is performed by (1) calculating two-way travel times for reflected P- and S-wave and one-way differential travel times between P- and S-wave for transmitted Sp-wave as a function of interface depth using actual ray parameter obtained from the earthquake source to station and earth model; (2) re-sampling of time series to an equal depth interval of 0.01 km; and (3) converting time series to a function of depth bring to realization of the NMO correction for reflections and transmissions.

Seismic Data Selection and Data Pre-processing

In the practice of earthquake data, we consider all aspects of parameters such as focal depth, epicenter distance, azimuthal variation, magnitude, and earth model. Earthquakes must be large enough to generate sufficient excitation of P- and S-wave reverberations beneath the station with high signal–to-noise ratio, so that direct and reverberating phases can be identified and their travel time differences can be calculated. We select events close to the station to assure relatively simple wave propagation paths and simple waveforms that NMO correction for reflections and transmissions can be better estimated. However, the station should also be located at sufficient distance to allow enough separation of reflected P-wave arrivals from Sp-wave arrivals converted at the base of the Cretaceous unconsolidated sediments and deeper interfaces. Based on the CERI standard velocity model, the basement reflection arrives at ~1.62 s after the primary P arrival on the vertical-component seismograms and at ~3.28 s after the primary SH arrival on the transverse-component seismograms. Sp conversions on the vertical-component precede direct S by 0.84 s. Also, event S-P time must be greater than 3s in order to resolve reflectors at about 4 km depth. Because well log data from Wilson 2-14 may not be the best to represent the unconsolidated sediments structure beneath stations and Paleozoic rocks may or may not be the Poisson's solids, small adjustments of Vp and Vs are allowed in the NMO migration process so that

reflection and transmission effects can be attributed to common major reflectors among P-, SH-, and Sp-wave.

The Seismic Analysis Code (SAC2000) (Goldstein and Minner, 1996) is used for data pre-processing to correct for DC offset and trend, remove instrument response, and integrate to ground displacement. A zero-phase trapezoidal bandpass filter is applied with frequency limits of 0.01, 0.1, 40, and 50 Hz. Then, two horizontal components are rotated along the great circle to radial (R) and transverse (T) orientations to facilitate the separation of P and SV from SH motions. We select time windows for P-wave (back to Sp) from Z-component and S-wave from T-component including their reflected waves. Zero-time is chosen at the peak of each phase. Sp-waveform is time-reversed with the peak of the direct SV-phase arrival being the zero-time from Z-component. We extract P-wave coda (back to Sp) and time-revered Sp-wave from Z-component and S-wave coda from T-component. Wave polarity is corrected such that firs-motion arrival is down to make the reflected and transmitted phases are in up-motion similar to the traditional reflection seismology. Time shift is determined by using cross-correlation between waveforms. Finally, all waves are corrected with respect to the zero-time reference at the peak of first pulse. Our idea is that stacking waveforms may be an effective approach to enhance energy of the reflected and transmitted waves and to suppress the scattering due to structural heterogeneity. In this manner, we can efficiently use this method widely for finding a first-order average velocity structure in the entire sediment column beneath the station.

Seismic Imaging Case Study: CUKY and HICK in southwestern Kentucky

We make use of pseudo-imaging profiling method to perform NMO corrections on the local earthquake waveform data including reflections and transmissions in an attempt to identify common reflectors and determine layered average velocity models in the deep sediments beneath two stations, CUKY and HICK, in southwestern Kentucky. CUKY is a broadband station co-sited at the top of the deep borehole CUSSO array operated temporarily by the University of Memphis. The depth of the borehole is known as 593 m. HICK is one of broadband stations of the Cooperative New Madrid Seismic Network (CNMSN). The thickness of the sediments beneath the station HICK, at Hickman, Kentucky, is about 584 m (Figure 1). Hick is located at 10 km east of CUSSO/CUKY. To minimize the level of the effects caused by laterally heterogeneous earth structure, we select events close to the station to ensure a better estimate of NMO corrections. Station locations and earthquake source parameters are listed in Tables 1 and 2. Detailed velocity model is constructed by using well log data from Wilson 2-14 and scaling to the depth of unconsolidated sediments beneath stations assuming a Nafe-Drake marine sediment model overlying a half-space Paleozoic rocks using acoustic log data from the Dow Chemical/Wilson #1 assuming Poisson's solid.

CUKY

Pre-processed displacement seismograms of three earthquakes (Figure 7a) are used in the pseudo-imaging analysis. We select time windows for P-wave (back to Sp) from Z-component and S-wave from T-component including their reflected waves. Zero-time is chosen at the peak of each phase. Sp-waveform is time-reversed with the peak of the direct SV-phase arrival being the zero-time from Z-component. We extract P-wave coda (back to Sp) and time-revered Sp-wave from Z-component and S-wave coda from T-component; correct their first arrival to the negative motions; and then stacking as shown in Figure 7b. Two-way travel time is calculated for P- and S-wave and one-way differential travel time between P- and S-wave is calculated for Sp-wave using a one-layer constant velocity model of Vp 2.0 km/s and Vs 0.6 km/s for unconsolidated sediments of 593 m thickness overlying a half-space of Vp 6.1 km/s and Vs 3.4 km/s for Paleozoic sedimentary rocks. Then, two-way and one-way travel times are re-sampled to an equal depth interval of 0.01 km. Figure 7c shows P- and S-wave coda with respect to two-way travel time and Sp-wave with respect to one-way differential travel time, extending to a depth of 5 km. Earthquake displacement travel time series are converted to a function of depth to implement NMO migration shown in Figure 7d and plotted for many times to form an imaging profiling for P-, SH- and Sp-wave (Figure 7e). Peak arrivals are at the zero reference time. All waveforms are in the negative

first motions and normalized to their individual maximum amplitudes within time or depth window shown in Figure 7(b) - 7(d). Thus, NMO migration seismic section is constructed using the velocity model mentioned earlier. Similar to traditional seismic reflection profile, Figure 7e shows that a strong reflector is correlated consistently to an interface at depth of 593 m corresponding to the upper Cretaceous/Holocene Mississippi Embayment Super Group (S) among all wave types. It also displays a common reflector in the deeper high-velocity section associated with Bonnerterre Formation Marker (B); however, it does not have a clear reflector associated with the low-velocity Elvins shale (E). Figure 7f re-plots imaging profiles for the top 593 m to depict the shallower reflectors within the unconsolidated sediments. Common reflectors can be seen at depths of 30, 100, 180, 225, 285, 400, 480, and 593 m that are similar to the results of the shallow reflection/refraction survey (Figure 8) conducted jointly by the University of Memphis and University of Kentucky (UoM/UKY) near the deep borehole site at CUSSO.

HICK

Hick is located at about 10 km east of CUSSO/CUKY in Kentucky. Given an average Vp of 2.0 km/s, S-wave arrival time, and sediment thickness of 584 m, an average velocity of S-wave in the whole sediment column is estimated as 0.6 km/s that is confirmed by the observed differential travel times between direct S and converted Sp waveforms among three earthquakes (Figure 9a). Imaging profiles are constructed by using a one-layer constant velocity model of Vp 2.0 km/s and Vs 0.6 km/s for the unconsolidated sediments of 584 m thickness overlying a half-space of Vp 6.0 km/s and Vs 3.4 km/s for Paleozoic sedimentary rocks to perform NMO corrections on the stacked displacement seismograms. Common reflectors in the deeper (Figure 9b) and shallower (Figure 9c) sediments come forth in the NMO migration imaging sections, which are similar to the results presented in Figure 7e and 7f for CUKY.

Transfer Function at CUSSO Borehole Array

The P-wave far-field displacement, D(t), for an earthquake source can be written in time domain as

$$D(t) = S(t)*E(t)*I(t).$$

where S(t) is the earthquake source time function; E(t) is the earth structure model; I(t) is the seismic instrument response; and '*' represents for convolution. We may re-write this equation in the frequency domain as

$$D(\omega) = S(\omega)\bullet E(\omega)\bullet I(\omega).$$

where $\omega = 2\pi f$ is the angular frequency and '•' represents for mathematical multiplication. Thus, amplification (modulus of transfer function) in unconsolidated sediments, A, can be written in frequency domain as

$$A(\omega) = D_s(\omega)/ D_b(\omega)$$

where $D_s(\omega)$ and $D_b(\omega)$ stand for displacement spectra from the surface and the base stations, respectively. P-wave coda is extracted from the vertical-component (Z) seismogram at the surface and at the base stations. Their amplitude spectra are calculated using Fourier Transform. Thus, the amplification (modulus of transfer function) for whole sediment column is the ratio of the amplitude spectrum at the surface station with respect to that at the base station. P-wave coda and its corresponding amplitude spectrum at the surface and at the base station as well as their spectra ratio are plotted in Figure 10. It shows that a peak amplification of 12 times is highly noticeable at frequency 20 Hz (green line), which is associated with the reverberated P-wave train of period 0.05 s within the near-surface soils. Similar analyses can be performed for stations at various depths as the CUSSO borehole array becomes fully operational. Observation of such large amplification associated with a high-frequency site response is vital to the environmental engineering and earthquake hazard assessment. A well-known relationship, T=4*D/V, says that the period (T) of reverberation can be controlled by the thickness of the layer (D) and a velocity in the layer (V) for constructive interferences of waves within a layer with opposite reflection

coefficients at top and bottom bounding interfaces. T is an observable from seismograms; the ratio of D/V is a useful constraint in waveform modeling for the near-surface structure; but not D or V simultaneously. We will address and model high frequency site response in a separate paper.

Transfer function time series can be obtained in the following procedures: (1) extract displacements from both the surface and the base recordings; (2) compute spectrum using Fourier Transform; (3) calculate spectral ratio; and (4) calculate transfer function time series using Inverse Fourier Transform. We extract waveforms starting at P- arrival for 1.9 s (back-to Sp) from the vertical-component (Z) seismogram for P-wave coda and starting at S arrival for 5 s from the transverse-component (T) seismogram for S-wave coda (Figure 11a). Two way travel times for P- and S-wave are calculated using a one-layer constant velocity model of Vp 2.0 km/s and Vs 0.6 km/s for unconsolidated sediments of 593 m thickness overlying a half-space of Vp 6.1 km/s and Vs 3.4 km/s for Paleozoic rocks. Then, time series are re-sampled into an equal depth interval 0.005 km and converted into a function of depth. Accordingly, we obtain transfer function time series in a function of two-way travel times (Figure 11b) and in a function of depth (Figure 11c) in the deep sediments for P- and S-wave. Figure 11d shows a NMO migration seismic depth section (same format as Figure 7e). Depth scale is the same on three panels in Figure 11. Common reflectors in sediments are identified and indicated by tick marks. It is interesting that a near-surface interface becomes noticeable at depth of 10 m, which may be associated with the thin low-velocity weathering soils and water table. According to the horizontal one-layer velocity model, the two-way travel times are calculated as 0.03 s for P-wave and 0.05 s for S-wave. This leads to average velocities of Vp ~667 m/s and Vs ~400 m/s in the top 10 m of horizontally layered soils for P- and S-wave at the site of CUSSO. Particular velocity model in the near-surface weathering zone is discussed in a separate paper; yet, this confirms that a gradient velocity model from surface down to 15 m will be sufficient in the Monte Carlo style global grid searching method to seek a reference model for near-surface soil structure in upper Mississippi Embayment (Chiu and Langston, 2011).

Discussions

Distinct seismic phases are excited at high impedance contrast boundary between the low-velocity sediments and high-velocity Paleozoic rocks; subsequently, these waves are confined within the low-velocity sediments to generate reverberations for P- and S- wave. For an earthquake with 7 km source depth and recorded at a station 12 km away, incidence angles for P and S waves are approximately 62º under the sedimentary layer and 12º and 9º within the sediment layer assuming standard CERI velocity model. Because the thickness of sediment is relatively thin compared to the depth of the earthquake source and velocities of sediments are extremely slow relative to that in the deeper region, there are little differences in ray parameters between phases produced by the P-wave (P, PpPhp, Ps) and between phases produced by the S-wave (S, SsShs, Sp). In the earlier numerical experiment, we found that vertical incidence two-way travel time calculation is a good approximation to the actual travel time for travel path in unconsolidated sediments. However, travel time curves for deeper reflectors deviate more from the reference curve at zero offset as offset increases (Chiu and Langston, 2009). It is also interesting to notice that moveout of the reflected (PpPhP and SsShs) phase is linearly proportional to the corresponding thickness of sediments, which provides an estimate of velocity within the unconsolidated sediments (Figure 12). In the first-order least-square fitting, this gives an average velocity of 2.0 km/s and 0.7 km/s for P- and S-wave, respectively, in the upper Mississippi Embayment. This result agrees with those from seismic reflection profiles (Hamilton and Zoback, 1982) and COCORP deep reflection survey (Nelson and Zhang, 1991) in the embayment.

Our study results in a simple one-layer constant velocity model of Vp 2.0 km/s and Vs 0.6 km/s for the entire column of unconsolidated sediments in southwestern Kentucky, which is confirmed by the observations of waveforms shown on the top and the bottom recordings in the CUSSO borehole array for P- and S-phase (Figure 5), as well as S-to-Sp differential travel times. It is exciting that PpP- and SsS-

phase are observed on the Z- and T-component seismograms at the base station from a local earthquake. Given the depth of CUSSO borehole array and the observed differential travel time between P- and PpP-phase as well as between S- and SsS-phase, it implies an average Vp 2.0 km/sec and Vs 0.6 km/s in sediments. However, Vs is higher than the direct measurements from the logging data (~0.4 km/s; Figure 4a). This could be due to improper casing at shallow depth that is common in the embayment environment. In addition, no reflector can be correlated with the low-velocity Elvins shale at depth about 2.8 to 3.2 km, which is similar to the absence of low-velocity layer at SP 1 (close to the CUKY and HICK) along profile 1-5-6 in a wide-angle reflection/refraction experiment conducted by Moony *et al*., (1983) and Ginzburg in 1983. Similar observation was also found beneath station PARM (Chiu and Langston, 2009), which may be due to the intrusion of Bloomfield pluton (see Figure 1) at depth about 2.5 - 3.5 km (Hildenbrand and Hendricks, 1995). More studies are needed to mapping the extent of the low velocity zone in the upper Mississippi Embayment.

This study confirms that the high frequency Sp-wave shown in Figures 7a & 9a are converted at the interfaces corresponding to the reflectors in the loose shallower sediments or at the base of the unconsolidated sediments, while relatively long-period Sp waves are converted at deeper interfaces in the Paleozoic sedimentary rocks. This implies that multiple Sp conversions are occurred at various depths beneath the Mississippi Embayment. The stretching features seen at deeper depths in the migration profiling is the nature of NMO corrections due to the large incident angle in the high-velocity Paleozoic materials, while P- and S-wave propagate upward near vertical incidence in the unconsolidated sediments.

Ground motions from local earthquakes seem to have been affected by the response of sedimentary structure to the incoming seismic waves. The characteristic resonant period (T = 4H/V) depends on the thickness (H) and velocity (V). It provides a very useful indicator to the dominant period of vibration at which the most significant amplification can be expected. Amplification (modulus of transfer function) becomes very large as resonance of the fundamental frequency (1/T) is met. As shown in Figure 2, the frequency-dependent site amplification is related to the earthquake magnitude as well as on the transfer modulus of the sediment column and the attenuation along the propagating path. Therefore, bulk density and velocity model including near-surface soil structure are of intrinsic interest in the estimation of earthquake hazard analyses and environmental engineering studies. The results of this research can be used to examine the nature and variability of high frequency site response in the range of 3-30 Hz band and to produce velocity models that can be applied to predict the low-strain seismic effects. Average velocity models for the entire embayment sedimentary column can be adopted to predict the relatively low frequency response (T=3~4 sec), which is important to the seismic response of large structures such as tall buildings and bridges. In other words, it will enable us to empirically examine the site-specific amplification of low-strain seismic waves independently from geotechnical field methods. The use of high- and relatively low-frequency earthquake waveforms can yield structure models of various resolutions, which, in turn, will elaborate upon wave reverberation effects and also can be employed to estimate site amplification for future strong ground motions due to large earthquake in the NMSZ. The use of these models in Probabilistic Seismic Hazards Assessments (PSHA) will place constraints on ground motion variability addressing uncertainty in the PSHA estimates. These direct applications of this research will contribute to reduce losses from earthquakes within the plate interior.

Conclusions

We exploit the pseudo-image profiling method to the local earthquake waveform data recorded by HICK and CUKY in an attempt to identify common reflectors and determine a velocity structure of the deep unconsolidated sediments beneath stations in southwestern Kentucky. Constrained by the differential travel times of $t_{P\text{-}PpPhp,}$ $t_{S\text{-}SsShs}$ and $t_{S\text{-}Sp}$, it suggests that the average velocity structure can be represented by a one-layer constant velocity model with Vp 2.0 km/s and Vs 0.6 km/s atop a half-space

Paleozoic sedimentary rocks of Vp 6.1 km/s and Vs 3.4 km/s. The sediment velocity model is consistent to the observations from waveforms recorded on the surface and at the bottom stations of the CUSSO borehole array. This study reaffirms the authenticity of pseudo-imaging profiling technique. Results from this study have indicated Vp/Vs ratios of 3.3 and 1.8 and Poisson's ratios of 0.5 and 0.3 for sediments and underlying rocks, respectively. It implies that Paleozoic rock is not a Poisson solid. Still, Vs (0.6 km/s) is higher than the direct well log measurements (0.4 km/s) at the CUSSO array. It casts doubts on the accuracy of the logging data. The spectral ratio taken from P-wave coda between the surface and the bottom stations in the CUSSO borehole array reveals that the P-wave is amplified by a factor of 12 at frequency 20 Hz; that is corresponding to the high-frequency reverberations at period of 0.05 s shown on the surface recording. This observation gives us a useful indicator of the dominant frequency of vibration to estimate the expected most significant ground amplification during future large shaking. Although deep borehole array is rare in the NMSZ or elsewhere, our study of limited borehole data find that low-velocity unconsolidated sediments in the upper Mississippi Embayment basin play important roles in wave reflections, transmissions, and amplifications. In comparison with the broadband observations on the basement, surface broadband seismograms provide essential data to enable exploration of effects of stratigraphic structure responses and accurate views of wave propagation mechanism. There is a near-surface reflector identified in the NMO migration seismic depth section at 10 m between P- and S-waves, which may be related to the near-surface weathering zone and/or water table.

Data and Resources

Software packages GMT (Generic Mapping Tool) (Wessel and Smith, 1998), SAC (Seismic Analysis Code) (Goldstein and Minner, 1996), and MATLAB were used in this study and are gratefully acknowledged. Seismic data were obtained from the CERI Seismic Data Archive. Data from the temporary deployment were submitted for archiving at the PASSCAL data center.

Acknowledgments

We would like to express our greatest gratitude to the anonymous reviewers for their detailed review, valuable comments and suggestions, which are incorporated in the manuscript. The Seismic Analysis Code (Goldstein et. al., 1996) and GMT (Wessel and Smith, 1998) are used for much of data processing, analyses, and preparing figures and are gratefully acknowledged. This research is supported by the U.S. Geological Survey, Department of Interior, under NEHRP grant award numbers G09AP00096 and G12AP20012 (University of Memphis) and G09AP000126 (University of Kentucky) and the Center for Earthquake Research and Information, University of Memphis. The views and conclusions contained in this document are those of the authors and should not be interpreted as necessarily representing the official policies, either expressed or implied, of the U.S. government.

References

Bäth M., and R. Stefansson (1966). S-P conversion at base of the crust. *Am. Geofis.*, 19, 119-130.

Bodin, P., K. Smith, S. Hortom, and J. Hwang, (2001). Microtremor observations of deep sediment resonance in metropolitan Memphis, Tennessee, *Eng. Geol*., 62, 159-168.

Catchings, R.D. (1999). Regional V_P, V_S, V_P/V_S and Poisson's ratios across earthquake source zones from Memphis, TN, to St. Louis, MO, *Bull. Seism. Soc. Am*., 89, 1591-1605.

Chen, K.C., J.M. Chiu, and Y.T. Yang, (1996), Shear-wave velocity of the sedimentary basin in the upper Mississippi Embayment using S-to-P converted waves, *Bull. Seism. Soc. Am*., 86(3), 848-856.

Chiu, S.C. and C.A. Langston, (2009). Reflection and transmission imaging of the upper crust using local earthquake seismograms, *Bull. Seism. Soc. Am*., 99(5), 3039–3054.

Chiu, S.C. and C.A. Langston (2011). Waveform Inversion for Near-surface Structure in the New Madrid Seismic Zone. *Bull. Seism. Soc. Am*., 101(1), 93-108.

Cramer, C., (2006). Quantifying the uncertainty in site amplification modeling and its effects on site-specific seismic-hazard estimation in the upper Mississippi Embayment and adjacent area. *Bull. Seism. Soc. Am*., 96, 2008-2020.

Dorman, J., and R. Smalley (1994). Low-frequency seismic surface waves in the upper Mississippi Embayment, *Seis. Res. Lett*., 65, 137-148.

Gao, F.C., (1999). High-resolution upper crustal P and S velocity structures in the upper Mississippi Embayment, MS thesis, the University of Memphis.

Ginzburg. A. W. D. Mooney, A. W. Walter, W. J. Lutter, and J. H. Healy., (1983). Deep structure of nothern Mississippi Embayment, *Am. Assoc. Petrol. Geol.* 67, 2031 – 2046.

Goldstein, P., and L. Minner, (1996). SAC2000: Seismic signal processing and analysis tools for the 21th century, *Seis. Res. Lett*., 67, 39.

Hildenbrand, T.G., and J.D. Hendricks (1995). Geophysical seting of the Reelfoot rift and relations between rift structures and the New Madrid seismic zone, *U.S.Geological Survey Professional Paper1538-E*, 30pp.

Langston, C.A., (2003). Local earthquake wave propagation through Mississippi Embayment sediments, Part I: Body wave phases and local site responses, *Bull. Seism. Soc. Am*., 93(6), 2671 – 2679.

Langston, C.A., P. Bodin, C. Powell, M. Withers, S. Horton, and W. Mooney, (2005). Bulk sediment QP and QS in the Mississippi Embayment, Central United States, *Bull. Seism. Soc. Am*., 95(6), 2162-2179.

Liu, H., Y. Hu, J. Dorman, T. Chang, and J. Chiu, (1997). Upper Mississippi Embayment shallow seismic velocities measured in situ, *Eng. Geol*. 46, 313-330.

Mclntyre, J., Z.M. Wang, E. Woolery, and G. Steiner, (2011). Instrumentation and Installation of the Central United States Seismic Observatory, presented at the SSA meeting, Memphis, TN. April 13-15, 2011.

Mooney, W.D., M.C. Andrews, A. Ginzburg, D.A. Peters, and R.M. Hamilton (1983). Crustal structure of the northern Mississippi Embayment and a comparison with other continental rift zones, *Tectonophysics*, 94, 327-348.

Nafe. J. E. and C. L. Drake (1957). Variation with depth in shallow and deep water marine sediments of porosity, density, and the velocities of compressional and shear waves, *Geophysics*, 22, 523-552.

NEHRP Recommended Provision for Seismic Regulations for New Buildings and Other Structures. FEMA-450-1/2003 Edition.

Nelson, K.D., and J. Zhang (1991). A COCORP deep seismic reflection profile across the buried Reelfoot rift, south-central United States, *Tectonophysics*, 197, 271-293.

Rix, G.J., G.L. Hebeler, and M.C. Orozco, (2002). New-surface Vs profiling in the New Madrid Seismic Zone using surface-wave methods, *Seism. Res. Lett.*, 73, 380-392.

Schneider, J.A., P.W. Mayne and G.J. Rix, (2001). Geotechnical site characterization in the greater Memphis area using cone penetration tests, *Eng. Geol.,* 62, 169-184.

Stearns, R.G., (1957). Cretaceous, Paleocence, and lower Eocenc geologic history of the southern Mississippi Embayment, *Geol. Soc. Am. Bull.*, 68, 1077-1100.

Street, R., E.W. Woolery, and J.M. Chiu, (2004). Shear-wave velocities of the post-Paleozoic sediments across the upper Mississippi Embayment, *Seism. Res. Lett*., 75(3), 390-405.

Vlahovic*, G.,* C. Powell*,* and J. Chiu, (2000). Three-dimensional *P* wave velocity structure in the New Madrid seismic zone, *J. Geophys. Res.,* 105, 7999 - 8012.

Wessel, P., and W.H.F. Smith, (1998). New improved version of the Generic Mapping Tools released, *Eos Trans*. AGU, 79, 579.

Williams, R.A., W.J. Stephson, A.D. Frankel, J. Odum (1997). Surface seismic measurements of near-surface P- and S-wave seismic velocities at earthquake recording stations, Seattle, Washington, *Earthquake Spectra*, 15(3), pp20.

Williams, R.A., S. Wood, W.J. Stephson, J.K. Odum, M.E. Meremonte, and R. Street (2003). Surface Seismic –refraction/reflection measurement determinations of Potential Site Resonances and the Areal uniformity of NEHRP Site Class D in Memphis, Tennessee: *Earthquake Spectra*, v.19, 159-189.

Author's Affiliations, Addresses
S-C. C. C.
C. A. L.
J-M. C.
Center for Earthquake Research and Information
University of Memphis, 3904 Central Ave.
Memphis, TN 38152

Z. W.
E. W.
Dept. of Earth & Environmental Sciences
University of Kentucky
Lexington, KY, 40506

Table 1. Parameters of Stations and Wells Used in this Study

Station Code	Latitude (N)	Longitude (W)	Depth (m)	Instrument
HICK	36.5409	-89.2288	23	CMG-40T
CUKY	36.5540	-89.3320	3	CMG6T
CUSSO	36.5540	-89.3320	593	
Paducah	37.0000	-88.7000		
Garigan	35.9038	-90.0342		
Haynes	35.8638	-89.8485		
Wilson 2-14	35.6584	-90.0983		
RISCO	36.5500	-90.0500		

Table 2 Parameters of Earthquakes used in the Imaging Process

Origin Time		Location		Depth	Magnitude
		Latitute (N)	Longitude (W)	(km)	
10/18/2006	20:58:20	36.54	-89.64	7.83	3.4
12/18/2009	11:38:09	36.45	-89.54	9.06	3.1
3/2/2010	19:37:35	36.79	-89.36	8.20	3.7
4/27/2010	08:42:33	36.50	-89.54	8.12	2.0
5/30/2010	02:34:02	36.55	-89.72	9.20	3.1

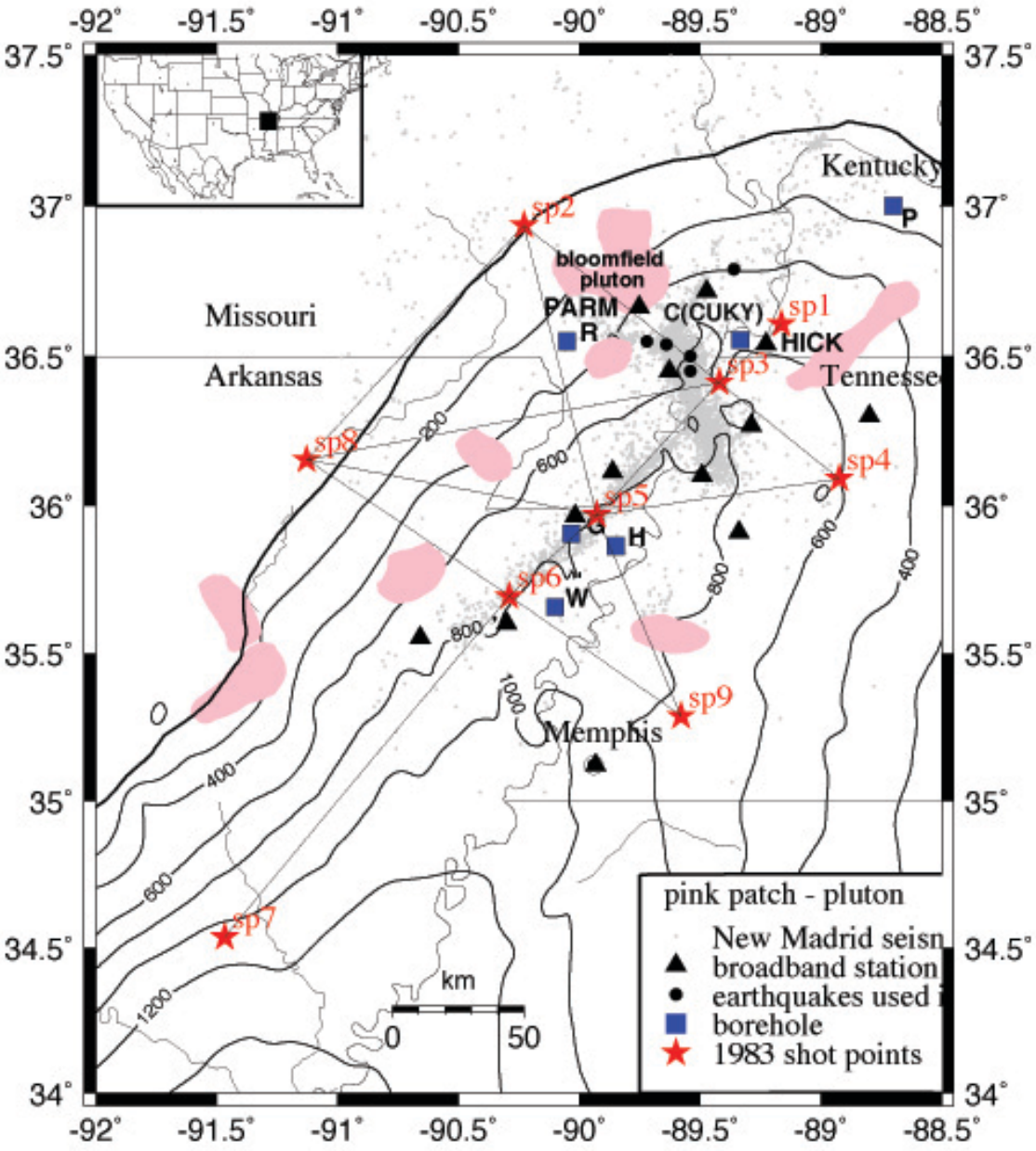

Figure 1. Location map. Contour lines represent the thickness of unconsolidated sediments in an interval of 200 meters with respect to the sea level for the upper Mississippi Embayment. Solid triangles are broadband stations of the Cooperative New Madrid Seismic Network operated by the University of Memphis. Solid square is the deep borehole well – CUSSO operated by the University of Kentucky, and other wells – Garigan (G), Haynes (H), Dow Chemical/Wilson #1 (W) in this region. The Wilson 2-14 well is located about 100 m from the Dow Chemical/Wilson #1 well. A temporary broadband station – CUKY was deployed at the top of the CUSSO during February 27 – June 25, 2010. Black circles represent the locations of earthquakes whose waveforms are used in this analysis. Upper left corner shows an index map and black rectangle represents our study area.

(a)

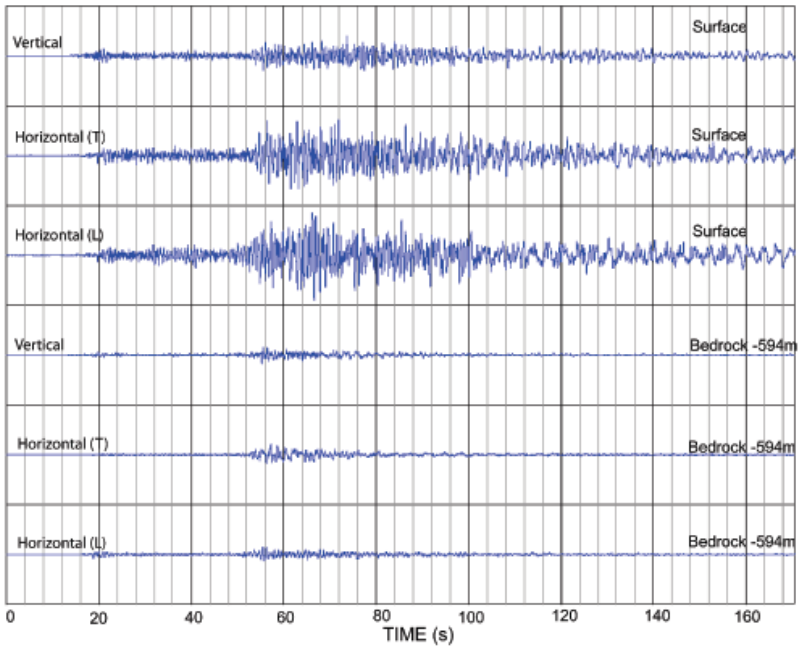

(b)

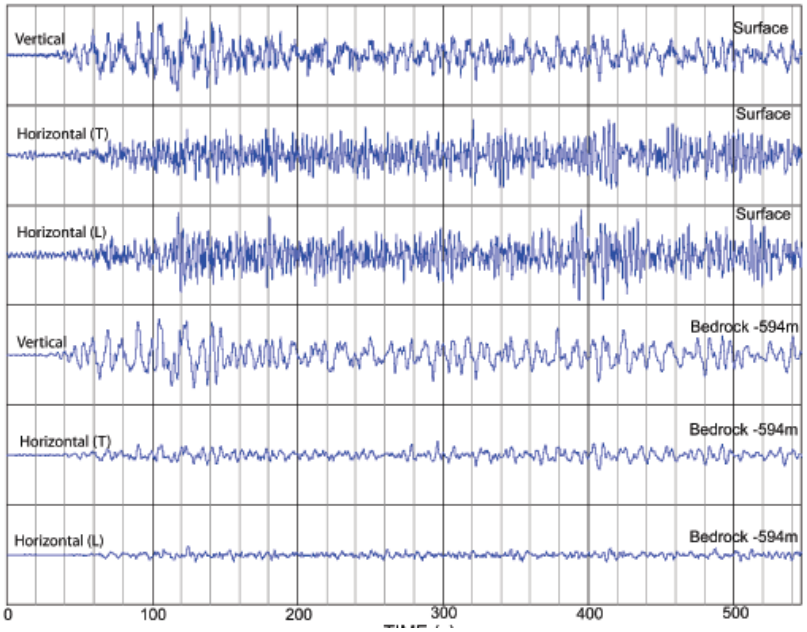

Figure 2. Waveform comparisons for the medium-period seismometer recordings at the surface and bedrock stations of the CUSSO borehole array showing (a). M 4.7 Greenbrier, Arkansas earthquake occurred on February 28, 2011; and (b). M 9.0 Japan earthquake occurred on March 11, 2011. Vertical scales within each diagram are the same. Time scale is in second and is different between (a) and (b). There are significant amplification and prolonging duration of ground motions (frequency dependent) at surface receivers as wave propagating from bedrock through unconsolidated sediments. Also, horizontal motions are affected more severe.

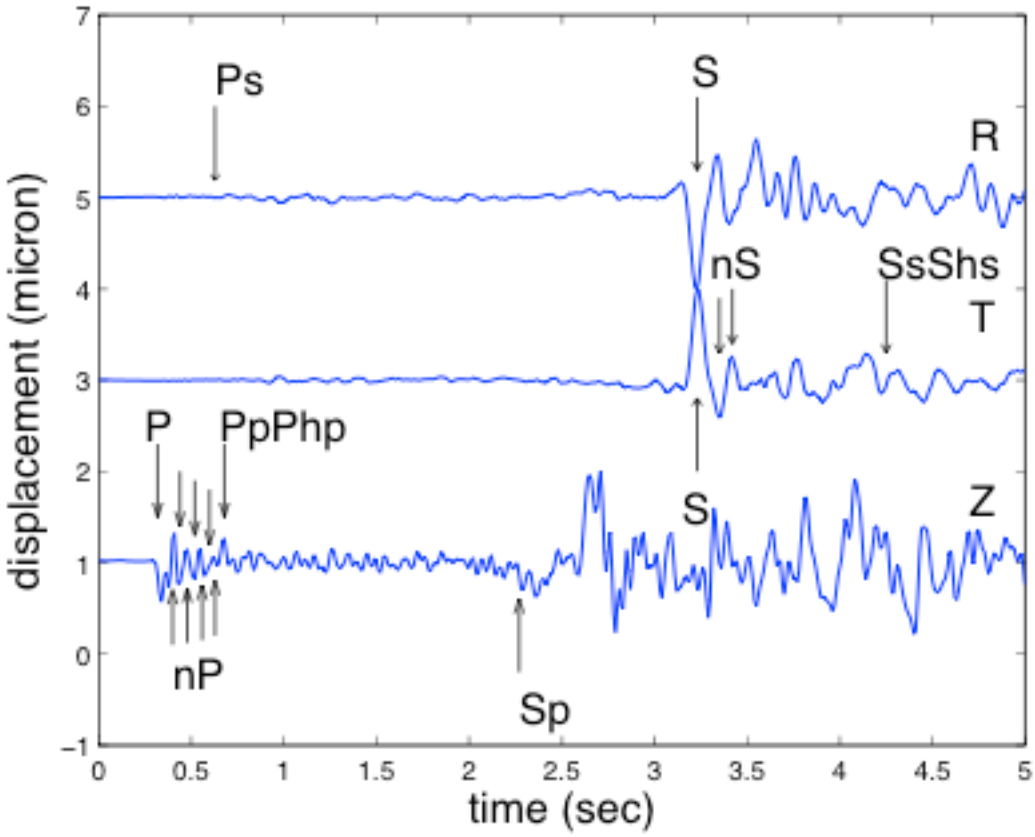

Figure 3. Typical example of displacement seismograms: a Md 2.0 Bassie. TN. earthquake occurred on April 27, 2010 @08:42:33.49. Ground motions are sampled at 100 samples/s for microearthquake recordings. The horizontal seismograms are rotated to radial (R) and transverse (T) components to facilitate the separation of P and SV motions from SH. Due to very low velocities and high Q in the unconsolidated sediments such that high frequency first reverberations of P and S (PpPhp and SsShs) waves can be observed and identified from the displacement seismograms. Major seismic phases are annotated. They are used to determine average velocities of P and S waves within sediments beneath the station. nP and nS are the resonate P- and S-wave in the near-surface soils.

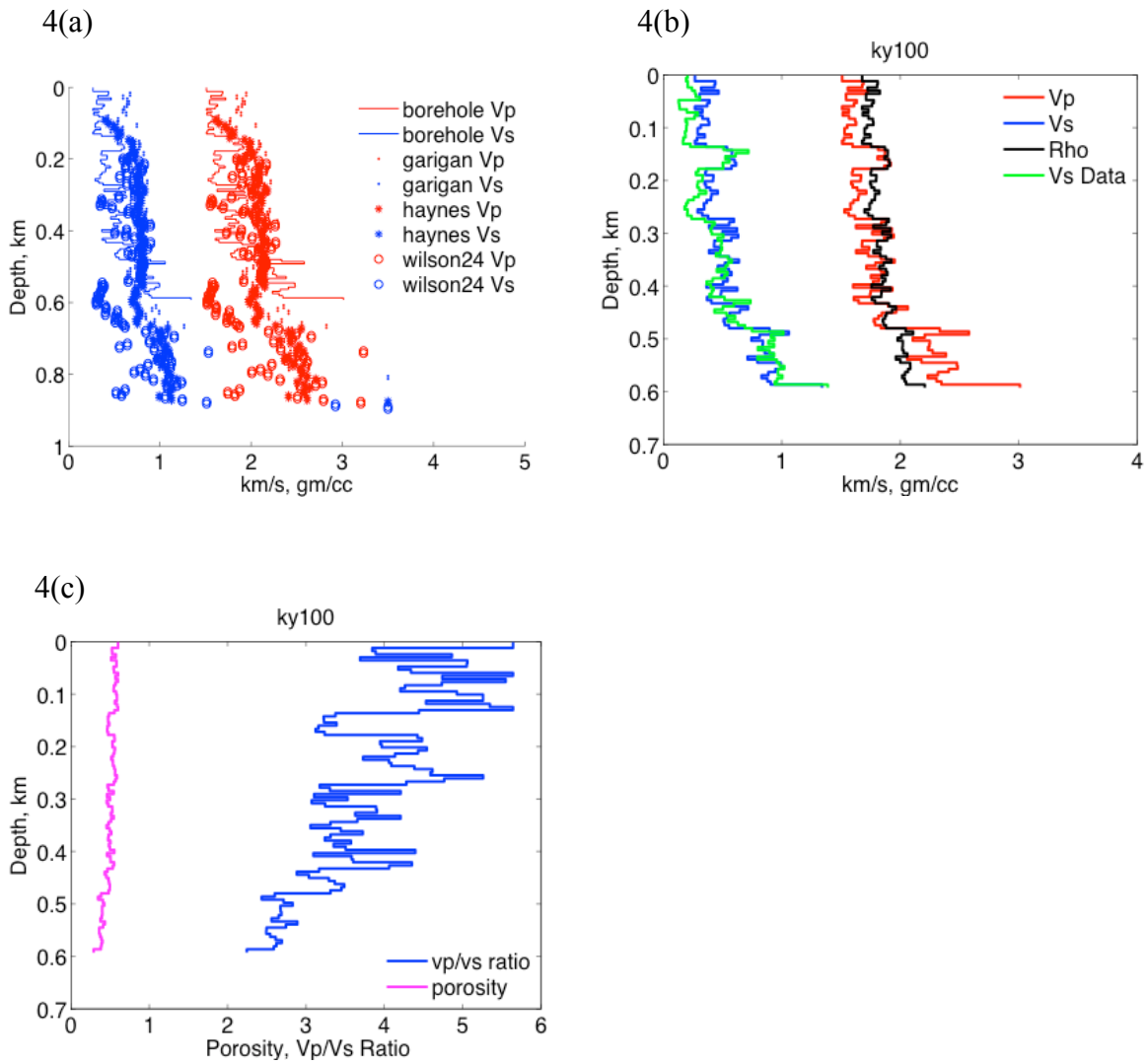

Figure 4. Well log information: (a) Collection of layered sediment Vp and Vs profiles among CUSSO, Garigan, Haynes, and Wilson 2-14. Vs is derived using the Nafe-Drake type sediment model except direct measurements used in the CUSSO well. It shows that the P-wave velocity variability is similar among four wells; though, the CUSSO Vs profile from direct measurements appears about half slower than others down to ~ 0.3 km; (b) Comparisons of direct measurements and derived S-wave (Vs_Data) velocities as well as derived density and direct measurements of P-wave velocity for the CUSSO; (c) Resulted Vp/Vs ratio and porosity in the CUSSO well.

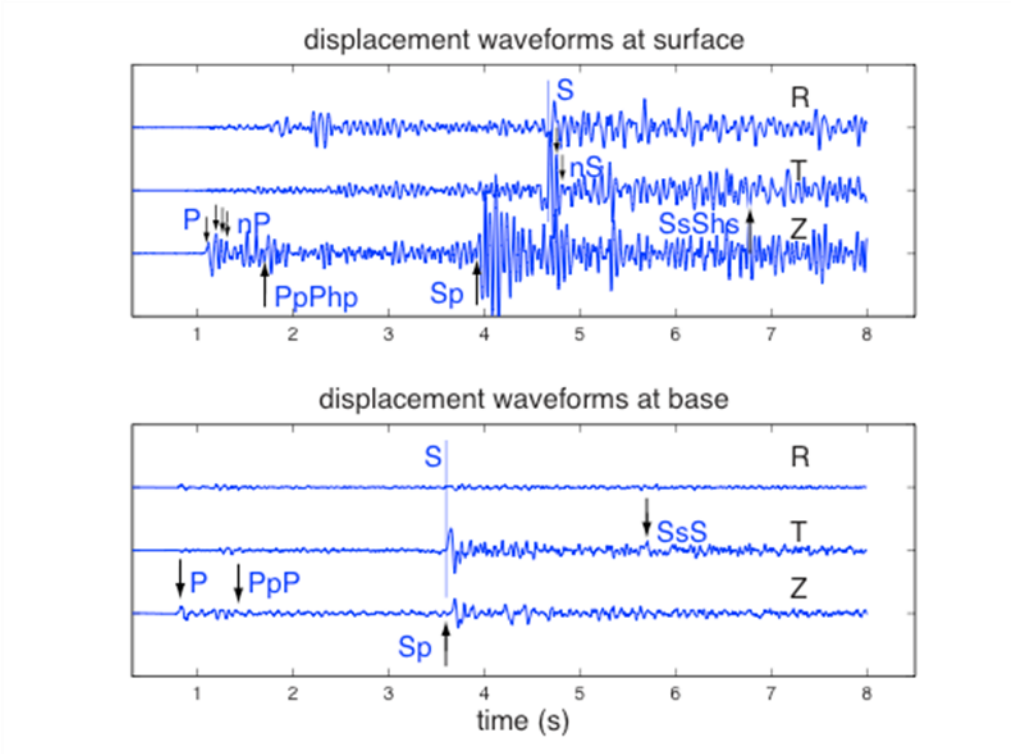

Figure 5. Displacement seismograms recorded at the surface and at the base of the CUSSO array indicated as ”C” in Figure 1. This is the Md 3.1 Point Pleasant, Missouri earthquake occurred on December 18, 2009 @11:38. Scales of ground motion and time are the same in both top and bottom figures. It is noticeable that ground motions are amplified and waveforms become much complicate as waves propagating through whole sediments section from the base of sediments. The horizontal seismograms are rotated to radial (R) and transverse (T) components to facilitate the separation of P and SV motions from SH. Top: surface recordings. nP and nS are high-frequency resonances P- and S-wave induced by the near-surface soils; Prominent energies of S and Sp phases should be considered in the earthquake hazards assessments. Bottom: base recordings. Down-going continuation of P- and S- wave (PpP and SsS) are observed at the Z- and T- component at the base of the array. Major phases are annotated.

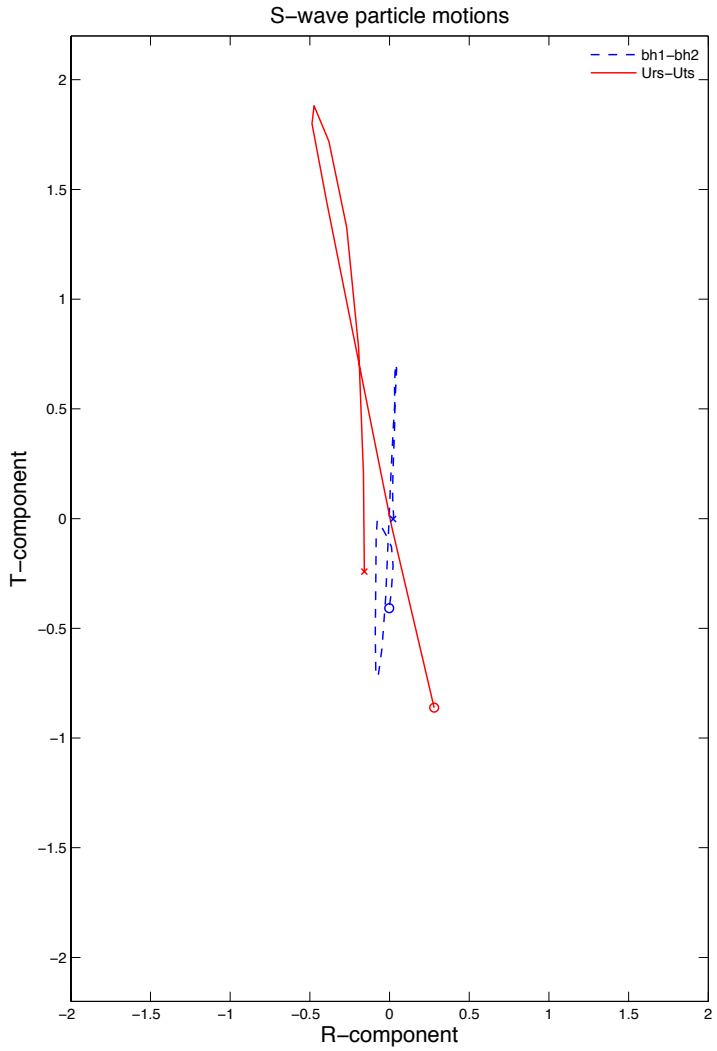

Figure 6. Comparison of S-wave particle motions between the surface and depth sensors. The surface horizontal-component data - sh1a (N-S) and sh2a (E-W) are rotated into the theoretical radial-direction (Urs) and transverse-direction (Uts) to facilitate the separation P- and SV motions from SH motions. It appears that bh1v, apparently, is in the radial-direction (R) and bh2v is in the transverse-direction (T) inside the borehole array as earthquake occurred. Clearly, magnitude of the S-wave particle motions become much larger and scattered at surface recording..

7(a)

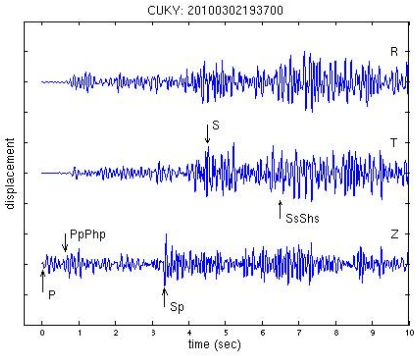

7(a)

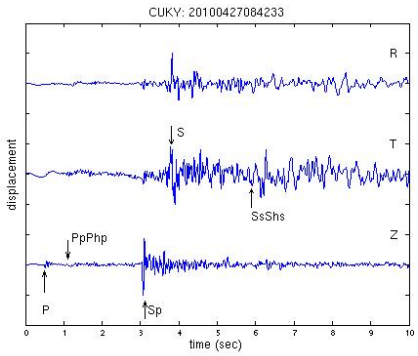

7(a)

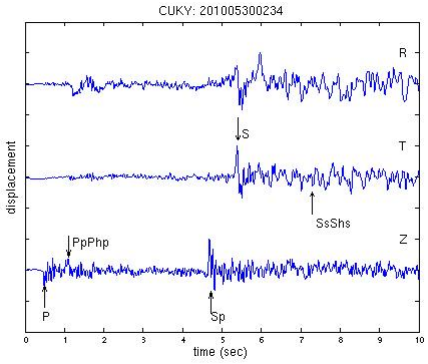

7(b)

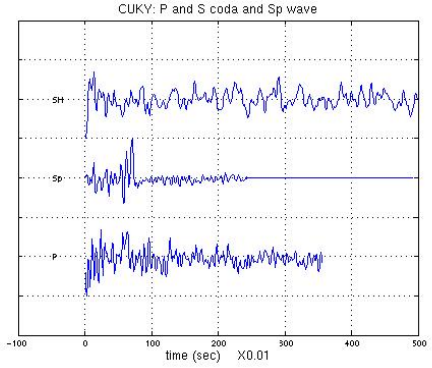

7(c)

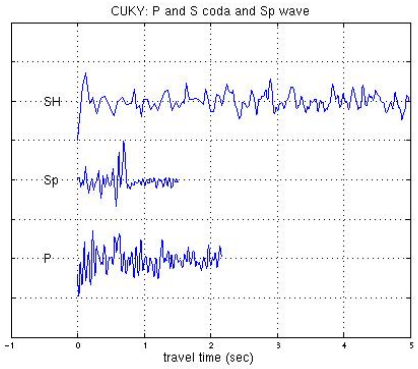

7(d)

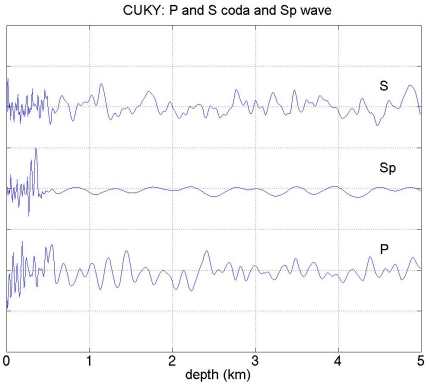

7(e)

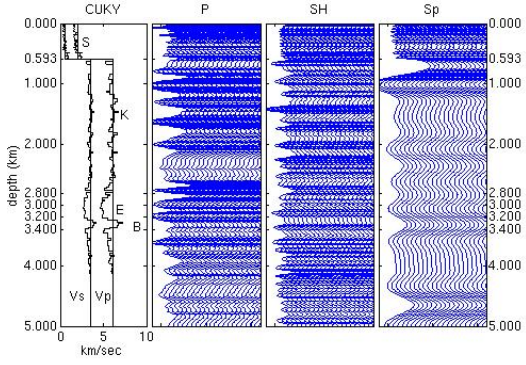

7(f)

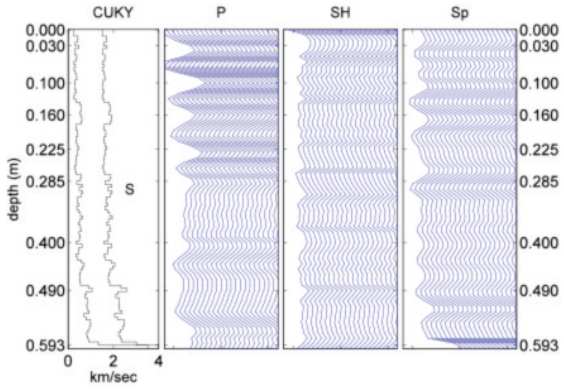

Figure 7. CUKY: Pseudo-imaging profiling. (a) Displacement seismograms of three earthquakes recorded at CUKY shown on radial- (R) and transverse- (T) and vertical- (Z) components. Major seismic phases are annotated; (b) coda of P- (back to Sp phase) and SH- waves, as well as Sp conversion wave; (c) NMO corrected P- and SH-wave coda and Sp conversions in a function of travel time, using a model of a constant velocity layer of Vp 2.0 km/s, Vs 0.6 km/s and thickness 583 m for unconsolidated sediments overlying a half-space of Vp 6.1 km/s and Vs 3.5 km/s for Paleozoic rocks; (d) Migrated P, SH, and Sp waves in a function of depth. P wave is shown at the bottom trace, Sp wave is at the middle trace, and SH is at the top trace for (b), (c) and (d); (e) NMO migrated seismic depth section. Strong reflectors appear at depths of 593 m and 3.2 km, which are associated with the Mississippi Embayment Super Group and Bonneterre Formation Marker, respectively. Letter-symbol representations are indicated by S for Mississippi Embayment Super group, K for Knox group, E for Elvins shale and B for Bonneterre Formation; (f) NMO migrated seismic section showing shallower structure within unconsolidated sediments extended to 0.6 km. Thick lines stand for average velocities and thin lines stand for detailed logging and derived data for P- and S-wave included in the left panel.

.

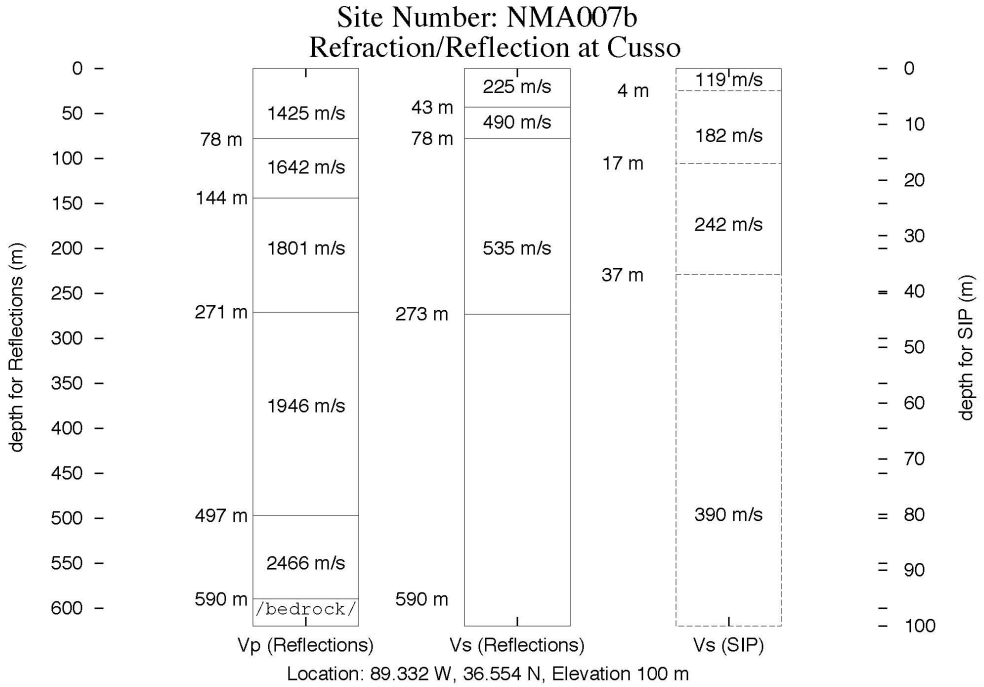

Figure 8. Velocity model for P- and S-waves resulted from the UoM/UKY reflection/refraction survey.

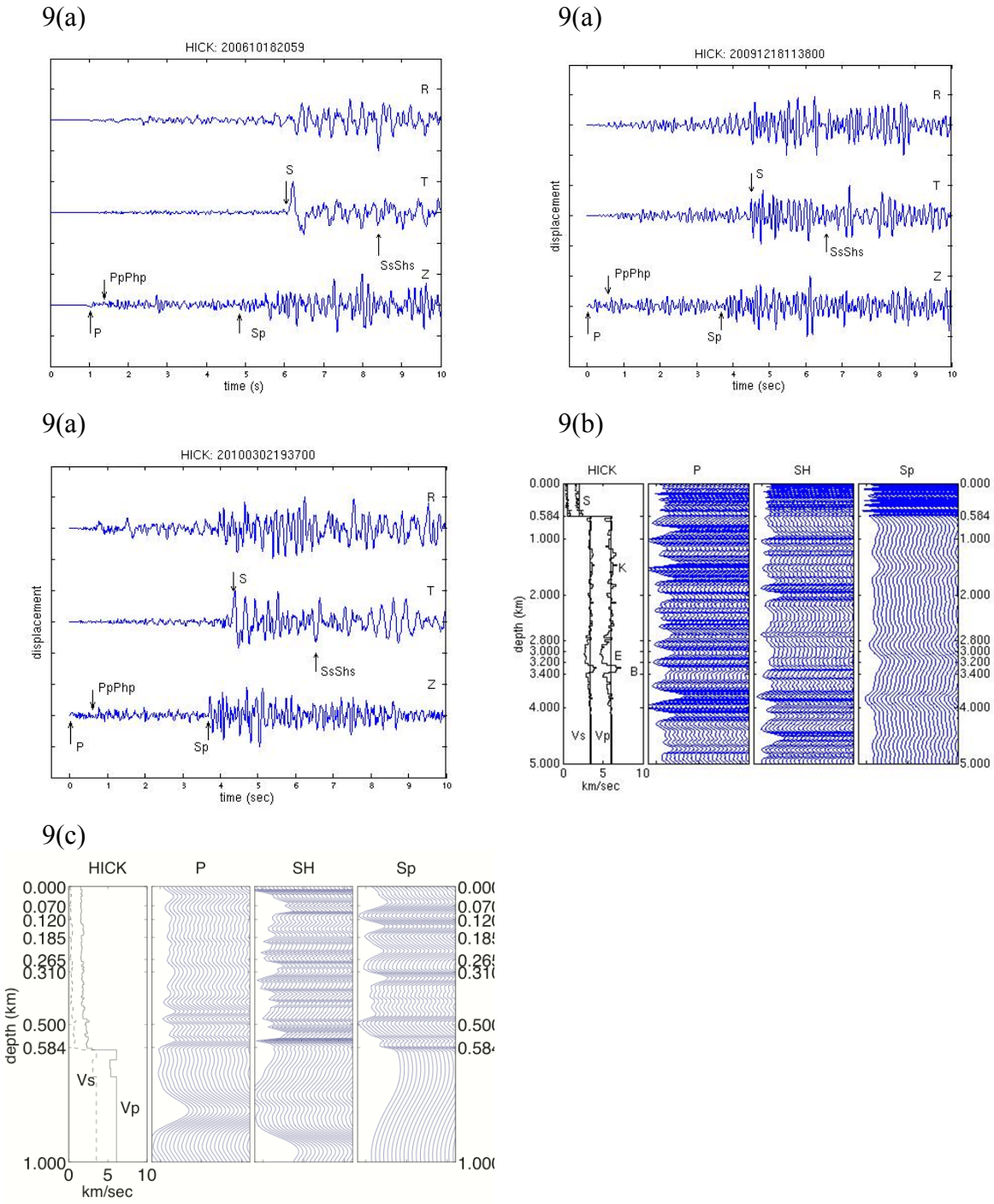

Figure 9. HICK: Pseudo-imaging profiles (same formats as (a), (e), and (f) in Figure 7). (a) Displacement seismograms (RTZ components) recorded at HICK for three earthquakes; Coda of P- and S- wave and Sp wave of their stacked waveforms are used in the imaging process. Major seismic phases are annotated; (b) NMO migrated seismic depth section constructed by using a constant velocity layer of Vp 2.0 km/s and Vs 0.6 km/s for unconsolidated sediments of depth 584 m overlying a half-space of Vp 6.0 km/s and Vs 3.4 km/s for Paleozoic rocks, extending to depth of 5 km; (c) NMO migrated seismic section of 1 km depth extracted from (b) for shallower unconsolidated sediments. Strong reflectors can be associated to S group at 584 m and Berreterre Formation similar to that in Figure (7e). Common reflectors are seen in depths of 70, 120, 185, 265, 310, 500, and 584 m.

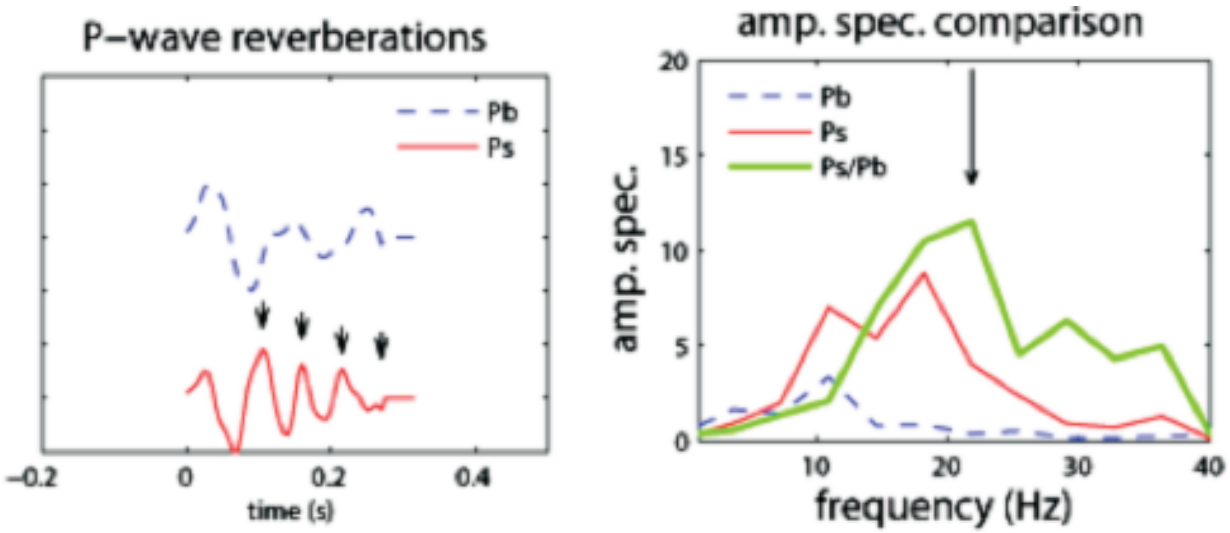

Figure 10. P-wave coda and spectra. (left): P-wave coda recorded at both the base (Pb) and the surface (Ps) stations; Both displacement amplitudes are displayed in the same scale. High-frequency near-surface reverberations indicated by arrows with time separation of 0.05s can be seen at surface recording that corresponds to the peak amplification on its amplitude spectrum shown to the right. (right): their individual amplitude spectra and corresponding spectral ratio. It shows that amplification of site response (amplitude spectral ratio) is increased to 12 times at frequency 20 Hz as marked by an arrow.

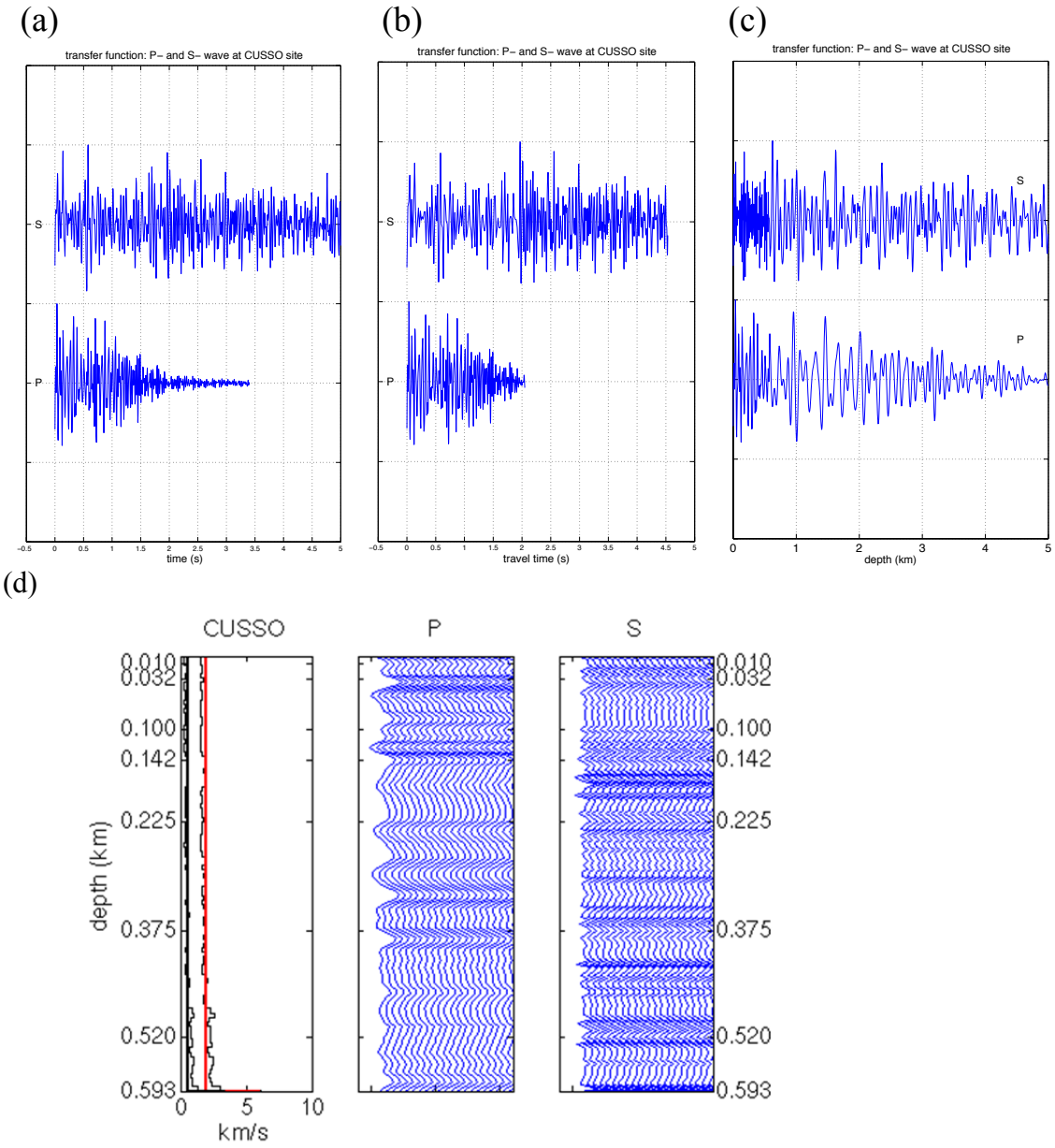

Figure 11. CUSSO: 1-D NMO migrated seismic depth section (same format as Figure 7e). (a) transfer function time series in deep sediments for P- and S- wave; (b) transfer function time series in a function of two-way travel times using using a 1-layer constant velocity model of Vp 2.0 km/s and Vs 0.6 km/s for unconsolidated sediments of 593 m thickness overlying a half-space Vp 6.1 km/s and Vs 3.4 km/s for Paleozoic rocks; (c) transfer function in a function of depth interval of 0.005 km extending to 5 km; (d) pseudo-imaging profiles in unconsolidated sediments for P- and S- wave. Common reflectors are indicated by tick marks between P- and S- wave. Note that a low-velocity near-surface interface appears at 10 m that may relate to the weathering zone.

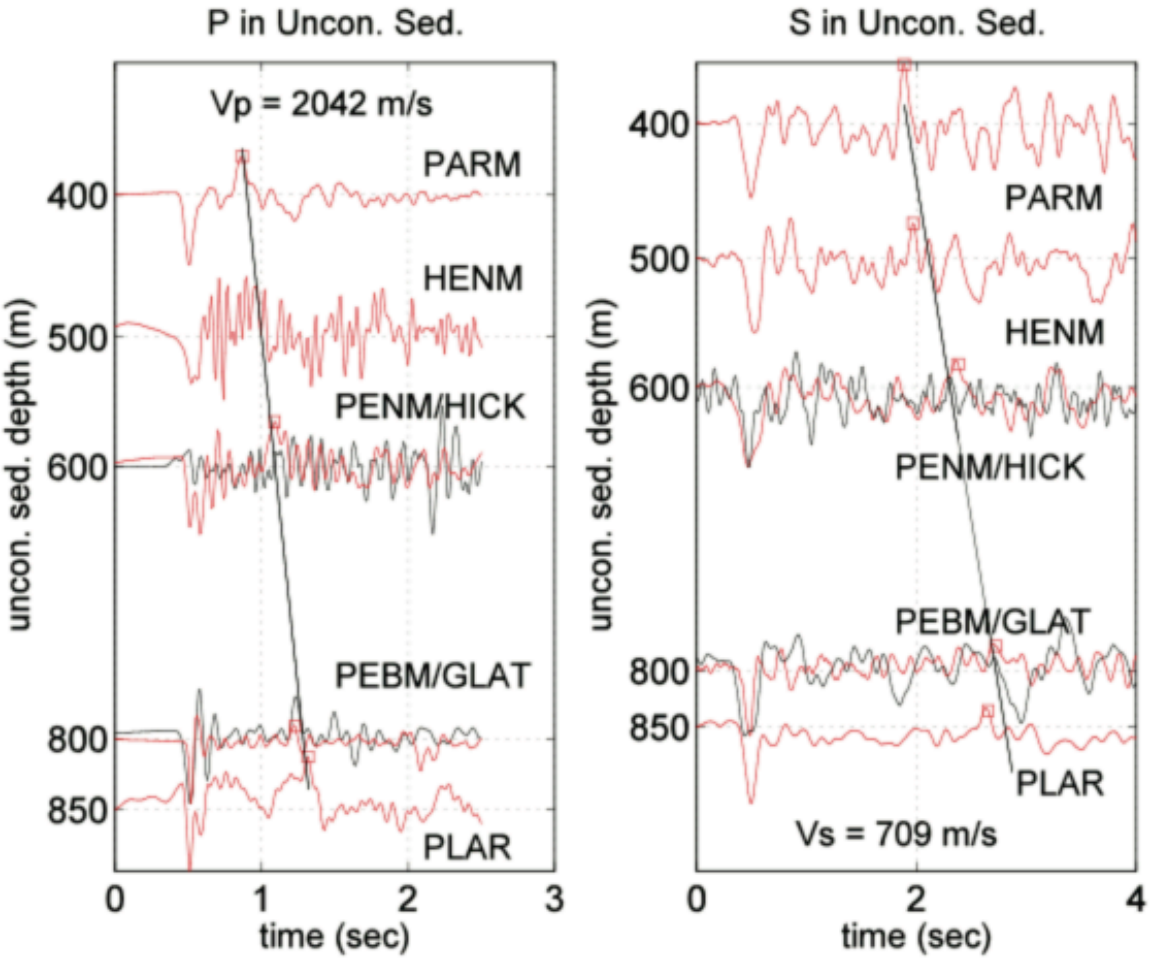

Figure 12. First-order velocity in the sediments using travel time moveouts of P- and S-wave reflections with respect to sediment depth. Squares indicate the arrivals of reflections (PpPhp or SsShs), respectively. 2.042 km/s for P-wave (a) and 0.709 km/s for S-wave (b) represent a velocity model for the unconsolidated sediments within the NMSZ. Station names are annotated.